Published in IEEE Journal of Selected Topics in Quantum Electronics 25, issue 4,
8800619, 2019 which should be used for any reference to this work

XUV Sources Based on Intra-Oscillator High Harmonic Generation With Thin-Disk Lasers: Current Status and Prospects

François Labaye, Maxim Gaponenko, Norbert Modsching, Pierre Brochard, Clément Paradis, Stéphane Schilt, Valentin Johannes Wittwer, and Thomas Südmeyer, *Member, IEEE*

(Invited Paper)

***Abstract*—Ultrafast thin-disk laser (TDL) oscillators provide higher intracavity pulse energy, average power, and peak power levels than any other femtosecond laser oscillator technology. They are suitable for driving extreme nonlinear interactions directly inside the laser oscillator. High harmonic generation (HHG) driven inside ultrafast TDL oscillators is a very recent approach for the generation of coherent extreme ultraviolet (XUV) light at multi-megahertz repetition rates. In this paper, we review the current state of the development, discuss the technological potential, and give an outlook toward the future developments. We compare the current performance to established technologies and evaluate possible limitations. We discuss future improvements, such as reduction of the driving pulse duration and increase of the intracavity peak power, efficient extraction of the XUV light from the cavity, and carrier-envelope offset frequency stabilization of the generated XUV light. Due to the power scalability of the TDL concept and the possibility to operate in a spectrally broadened regime with pulse durations below the gain bandwidth limitation, intra-oscillator HHG with TDLs has a high potential for powerful table-top multi-megahertz coherent XUV light sources for science and applications.**

***Index Terms*—Mode-locked lasers, high-power lasers, nonlinear optics, XUV sources.**

I. Introduction

COHERENT extreme ultraviolet (XUV) light sources have led to many advances in various scientific areas such as X-ray imaging [1], [2], biology and biochemistry [3]–[5], or studies of electrons dynamics [6], [7]. This variety of applications calls for the development of table-top XUV light sources.

Manuscript received October 24, 2018; revised June 24, 2019; accepted June 26, 2019. Date of publication July 1, 2019; date of current version August 5, 2019. This work was supported in part by the European Research Council Starting Grant 2011 under Grant 279505, in part by the Swiss National Science Foundation (SNSF) R'equip Project "OPTICS: Optical Ibs Coatings For Swiss Research" under Grant 206021_144970, and in part by the SNSF Project under Grant 200020_179146. *(Corresponding author: François Labaye.)*

The authors are with the Laboratoire Temps-Fréquence, Université de Neuchâtel, CH-2000 Neuchâtel, Switzerland (e-mail: francois.labaye@unine.ch; maxim.gaponenko@unine.ch; norbert.modsching@unine.ch; pierre.brochard@unine.ch; clement.paradis@unine.ch; stephane.schilt@unine.ch; valentin.wittwer@unine.ch; thomas.sudmeyer@unine.ch).

Color versions of one or more of the figures in this paper are available online at http://ieeexplore.ieee.org.

Digital Object Identifier 10.1109/JSTQE.2019.2926024

The most successful approach is based on high harmonic generation (HHG) [8], [9]. HHG is a highly nonlinear process that is typically driven by intense femtosecond laser pulses focused onto a gas target. High peak intensities ranging from a few 10^{13} W/cm^2 to a few 10^{14} W/cm^2 are usually required to achieve the up-conversion of the driving laser frequency to its higher harmonics. Nowadays, table-top sources based on this principle deliver spatially [10] and temporally [11] coherent XUV and soft X-ray light [12]–[14]. Furthermore, HHG also enables the generation of attosecond-scale pulses [15]–[17] and have the potential to reach even shorter pulse durations [18]. Applications of HHG enabled numerous break-through results in, e.g., chemistry [19], [20], XUV metrology [21], [22] or studies of ultrafast electron dynamics [23]–[25].

Whereas the HHG process was discovered about thirty years ago [8], [9], a strong development towards high-flux table-top HHG sources is still ongoing. Standard HHG systems typically rely on Ti:sapphire chirped pulse amplifiers. They usually operate with ultrashort pulses with multi-millijoule energy, but are limited to kilohertz repetition rates and average powers of a few watts [26]. Many applications would strongly benefit from higher repetition rates. For example, in experiments such as electron–ion coincidence spectroscopy [27], [28], photoelectron spectroscopy [29]–[32] and microscopy [24], the energy or momentum of photoelectrons has to be precisely measured. If too many photoelectrons are simultaneously created during a single excitation pulse, space charge effects (electromagnetic forces between the generated charged particles) may blur the resolution [33]. Achieving sufficiently high signal-to-noise ratio from quasi-single ionization events requires integration over a large number of events. Therefore, increasing the repetition rate from kilohertz to megahertz can result in a strong decrease of the measurement time.

A second limitation is the low flux of typical HHG sources. The highest conversion efficiency for the HHG process (between the infrared driving source and one harmonic) is currently 7.5×10^{-5} [34], whereas standard systems operate rather at a level of 10^{-7}–10^{-6}. Therefore, typical average infrared driving powers of a few watts from Ti:sapphire chirped pulse amplifiers will only lead to nW-μW of XUV average power. The limited

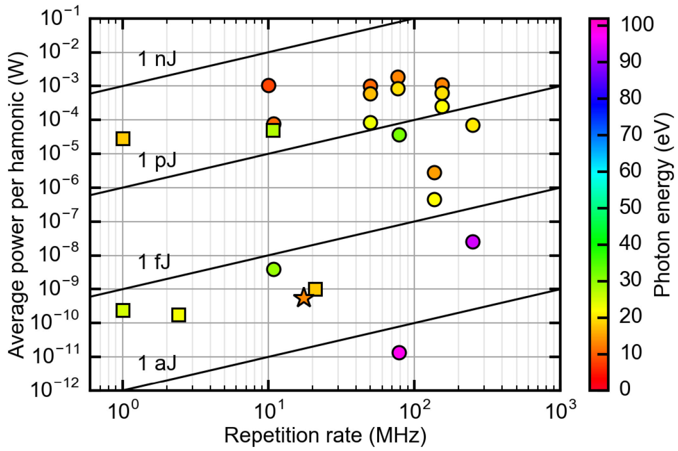

Fig. 1. Overview of XUV light sources based on HHG in gases operating at megahertz repetition rates. Symbols represent the applied approach (single-pass in squares, fsEC in circles, and intra-oscillator with a star). If the generated power was not reported by the authors, we estimated it using known extraction efficiency values. Data from: [22], [37]–[50].

photon flux is an issue for applications such as high resolution imaging, because it strongly affects the acquisition time and resolution [35], [36]. Moreover, other applications like frequency comb spectroscopy [21], [22] require both megahertz repetition rates in order to obtain a well-resolved optical frequency comb and a higher average power to have a sufficient power per comb line.

During the last decade, these challenging requirements connected with the large potential for scientific applications has led to significant research efforts towards the development of table-top high-flux XUV light sources based on HHG at megahertz repetition rates. Fig. 1 shows an overview of the achievements in XUV light generation at megahertz repetition rates.

In order to increase the repetition rate from kilohertz to megahertz while keeping the peak power high enough to drive the HHG process, the average power of the driving laser needs to be increased accordingly. One very successful approach is switching from green-pumped Ti:sapphire laser systems to diode-pumped solid-state laser (DPSSL) architectures allowing for average powers of ten to multi-hundred watts in sub-picosecond pulses. Systems based on coherently-combined fiber chirped-pulse-amplifiers (CC-FCPA) [51], [52], slab lasers [53] and ultrafast thin-disk laser (TDL) oscillators [54]–[57] respond to these requirements. These laser systems already demonstrated single-pass HHG at megahertz repetition rates [39]–[42] with average power of a few tens of microwatts down to 41 nm (25th harmonic, 30.2 eV) at 10.7 MHz [41] and have been used for high-speed coherent imaging [36], [58] and coincidence experiments [59] at repetition rates of 100 kHz or lower. However, achieving sufficiently short pulse durations for an efficient HHG process required a nonlinear pulse compression [60], [61].

An alternative approach to push the performance of HHG to higher XUV light fluxes is the use of femtosecond enhancement cavities (fsEC). It allows increasing the average and peak powers by coherent addition of optical pulses from a mode-locked laser in a passive optical cavity [62]. This approach leads to an intracavity peak power enhancement by factors ranging from 100 to 10,000, enabling a few kilowatts of intracavity average power to be reached using only an ultrafast laser with a few watts of average power. Without HHG process, this technology resulted in the realization of light sources with an intracavity average power up to 400 kW in 250-fs pulses [63]**.** Placing the gas target directly inside a fsEC allowed for HHG at megahertz repetition rate for the first time in 2005 [37], [64]. If the driving laser is an optical frequency comb (i.e., if its two degrees of freedom, the carrier-envelope offset frequency (f_{CEO}) and the repetition rate f_{rep}, are stabilized), this approach generates an XUV frequency comb at each harmonic. This was used for the first direct frequency comb spectroscopy experiment in the XUV [22], and a coherence time longer than 1 s was reported [11]. HHG in fsEC allowed for the generation of XUV light with photon energies exceeding 100 eV at a repetition rate of 250 MHz [47] and for photoelectron spectroscopy without space charge effect [32]. Furthermore, a careful optimization of the phase-matching recently enabled the generation of average powers up to ∼1.9 mW at 97 nm (11th harmonic, 12.8 eV) and ∼0.87 mW at 63 nm (17th harmonic, 19.7 eV) at repetition rates of several tens of megahertz [50] at repetition rates of several tens of megahertz. As the XUV beam in all of these experiments is collinearly propagating with the intracavity infrared beam, it is important that the XUV extraction method does not compromise the cavity enhancement. Initially, the out-coupling of the XUV light was simply done using a sapphire window placed under Brewster's angle for the driving laser wavelength, the difference in refractive index between the driving field and the XUV light allowing for some reflection in the XUV [37], [64]. In 2008, a novel approach was demonstrated using an XUV grating etched on top of a dielectric intracavity mirror [38]. While its out-coupling efficiency is moderate, the XUV beam is spectrally separated, so that a single harmonic can easily be selected for further experiments. Another alternative is the holey mirror technique which was first suggested by Moll and co-authors [65] and successfully implemented by Pupeza and co-authors [45]. Additionally, several other methods have been proposed to extract the XUV light, such as non-collinear HHG [66], [67], AR-coated plates [68] or a low-loss VIS/IR-XUV beamsplitter [69]. However, they have not yet been implemented for HHG driven by fsEC.

The required peak intensities for HHG are also achievable inside state-of-the-art femtosecond mode-locked lasers. Thus, a promising alternative to the previously described methods is to exploit the extreme nonlinear process directly inside the cavity of such laser oscillators. This approach is similar to fsEC in the sense that the intracavity average and peak powers are strongly enhanced compared to the values at the laser output. Additionally it does not require any further amplification or nonlinear pulse compression as in the single-pass architecture. However, unlike to fsEC, no coherent coupling of the seed light in an external optical resonator is needed. Furthermore, as it will be discussed in Section III-D, the plasma-induced nonlinearities that can have an effect in fsEC [70]–[72] are expected to be mitigated by the self-phase modulation (SPM) already introduced for soliton mode-locking [73]. A first proof-of-principle demonstration of intra-oscillator HHG reported in 2012 was

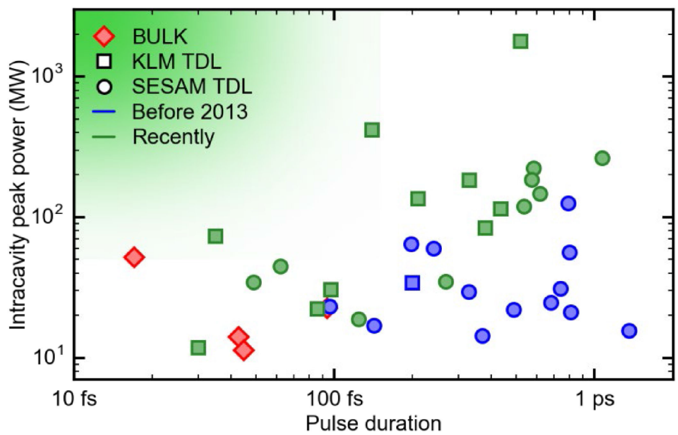

Fig. 2. Selection of Yb-based bulk laser and TDL oscillators operating with more than 10 MW of intracavity peak power, reported as a function of their pulse duration and intracavity peak power. For TDLs, a distinction is made between systems developed before 2013 (blue) and after (green). Data from: [54]–[57], [74], [78]–[103].

based on a Ti:sapphire laser oscillator [74]. The authors claimed the detection of photons with energies up to 30–40 eV. However, the intracavity average power was limited to 10 W. This is a major challenge to overcome in this approach if a high-flux XUV light source is targeted as the laser oscillator needs to operate with an average intracavity power in the range of 0.1–1 kW or more and to generate femtosecond pulses. The bulk oscillator approach does not seem to be suitable for high-flux XUV light sources as a result of limiting effects such as damage of the laser crystal and strong thermal lensing in gain materials that prevents laser power scaling. This is not the case for TDL oscillators, which are based on a power-scalable concept [75], [76]. The gain medium has the shape of a thin disk (typically with a thickness of 100–200 µm), which is mounted onto a heat sink and used in reflection with a large beam diameter [54], [75]. The thin-disk geometry enables efficient cooling of the gain crystal, thus limiting thermal lens aberrations, and strongly reduces nonlinearities in the gain element.

The first continuous-wave (cw) diode-pumped TDL oscillator reported in 1994 already achieved an intracavity average power of more than 300 W using a few watts of pump power [75]. Today, intracavity average powers up to 135 kW in cw operation with only 54 W of pump power have been demonstrated and further power-scaling to megawatt level was predicted [77]. Mode-locking of TDL oscillators for the generation of ultrafast laser pulses was achieved in 2000 [54]. Nowadays the intracavity peak power has been increased up to 1.76 GW [78]. Modern ultrafast TDL oscillators deliver the highest average power and pulse energy of any mode-locked laser oscillators technology, both intra- and extra-cavity [55], [56], [79], [80]. Fig. 2 shows the evolution of the intracavity peak power and pulse duration of Yb-based bulk laser and TDL oscillators over the last two decades. The trade-off between intracavity peak power and short pulse duration has been overcome in the last five years. Today, intracavity peak powers in the order of multi-hundreds of MW have been obtained with sub-150-fs pulses [57]. Pulse durations as short as 30 fs were demonstrated [81] from diode-pumped Yb-doped gain materials. This performance makes TDL oscillators ideal candidates for applications of intra-oscillator extreme nonlinear optics and a suitable base for the development of high-flux table-top XUV light sources at megahertz repetition rates based on HHG.

In this review article, we first give an overview of the current status of XUV light sources based on intra-oscillator HHG with TDLs [49], [104], [105] in Section II. Then, we discuss in Section III the current technological limitations and the required developments to overcome them. In Section IV, the suitability of intra-oscillator HHG with TDLs for the realization of XUV optical frequency combs is discussed. Finally, an outlook towards applications and future research directions is given in Section V.

II. Intra-Oscillator HHG With Mode-Locked TDLs

A. *General Requirements for Intra-Oscillator HHG*

The realization of a mode-locked TDL oscillator suitable for intracavity HHG requires the combination of several technical parameters listed below, which are addressed by the development of advanced cavity concepts.

- The oscillator has to be optimized for high intracavity average and peak powers in combination with a short pulse duration and long-term stability. The employed mode-locking method has to support this operation regime.
- Optical elements providing negative dispersion in proper combination with SPM have to be introduced in the cavity for soliton mode-locking operation.
- The resonator design requires an additional tight intracavity focus (beam radius of 10–20 µm in the current systems) to reach the peak intensities needed for the HHG process at megahertz repetition rates. Strongly focusing curved mirrors used in an improper cavity design may lead to a severe astigmatism, which can prevent operating in a single transverse mode.
- Thermal effects can be a severe issue in high-power TDL oscillators. Power-dependent thermal lenses and aberrations can potentially be introduced not only by the gain element, but also by other intracavity components such as dispersive mirrors. Therefore, advanced cavity designs are required, which provide well-defined beam sizes on the key optical components to achieve single-transverse mode operation and stable cw-mode-locking.
- The cavity sensitivity to mechanical misalignments must be minimized. Whereas this is always beneficial in any laser oscillator, it is even more crucial here since it also affects the pointing of the XUV beamline, which in turn would impact any downstream experiment.

As previously mentioned in the introduction, intra-oscillator HHG implemented within a TDL is in some aspects very similar to the use of a fsEC and, as such, has also many similar requirements:

- The optical cavity needs to have moderate losses in order to provide sufficient enhancement for efficient laser operation at reasonable pump power levels.

- The extraction of the generated XUV light from the oscillator cavity should be as efficient as possible while being the least intrusive to the driving oscillator.
- The strong absorption of the generated XUV light in ambient air makes it necessary to operate the oscillator in a vacuum environment under a maximum residual pressure of 10^{-2} mbar.
- Finally, to generate an XUV frequency comb, a stabilization of both the CEO frequency $f_{\rm CEO}$ and of the repetition rate $f_{\rm rep}$ of the TDL oscillator has to be implemented.

B. *Current Status*

Intra-oscillator HHG with TDLs is still a technology in an early development stage. The first demonstration was done in 2017 [49], [104], and so far only two research teams have reported this approach. The first system was based on a ultrafast TDL oscillator mode-locked by a SEmiconductor Saturable Absorber Mirror (SESAM) [106]. It employed an $Yb:Lu_2O_3$ gain medium and operated at a repetition rate of 17.35 MHz. The focus of this work was the proof-of-principle demonstration of a compact and simple XUV light source based on intra-oscillator HHG within a TDL, which resulted in the generation of XUV light down to 60.8 nm (17th harmonic, 20.4 eV). This system will be discussed in details in the next sections. The second system has so far only been reported in a conference article [105]. The authors developed the concept of a photon ring with multiple HHG ports, allowing for the generation of several XUV light beam lines operating at the same time for multi-user or multi-color experiments. Therefore, the system has a larger size and a repetition rate of only a few megahertz. It is based on a Kerr-lens mode-locked (KLM) Yb:YAG TDL oscillator. It operates with two intracavity HHG ports at a repetition rate of 3.11 MHz with an intracavity peak power of 519 MW, a pulse energy of 0.36 mJ, a pulse duration of 610 fs, and an intracavity average power of 1.12 kW [78]. The radius of the tight focus at each port is assumed to be $\sim$15 µm, which leads to an estimated peak intensity of 8.4×10^{13} W/cm^2. In the first HHG port, neon was used as gas target for XUV light generation down to 24 nm (43th harmonic, 51.7 eV), while argon was used in the second port for XUV light generation down to 49.1 nm (21th harmonic, 25.3 eV).

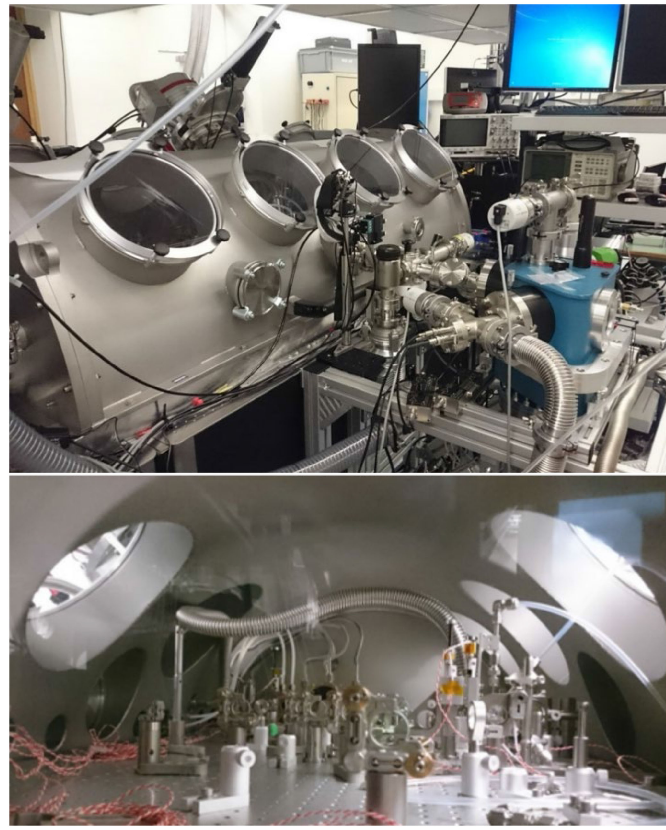

Fig. 3. Pictures showing external (top) and internal (bottom) views of the vacuum chamber enclosing the TDL oscillator for intra-oscillator HHG.

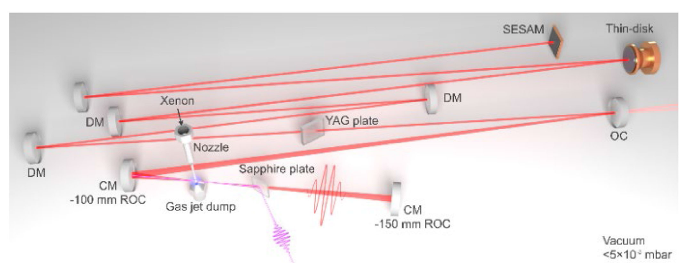

Fig. 4. Scheme of principle of intra-oscillator HHG with TDL (DM: dispersive mirror; CM: concave mirror; ROC: radius of curvature; OC: output coupler). Reprinted with permission from [49].

C. *SESAM-Mode-Locked TDL for Intra-Oscillator HHG*

In the following sections, we present a summary of the intra-oscillator HHG system reported in [49] and discuss specific aspects of the chosen design, which have not been reported so far. This will then serve as a baseline to discuss guidelines towards reaching a high-flux XUV light source based on intra-oscillator HHG with TDL oscillators.

The optical resonator, the TDL head, and the gas target are enclosed in a compact vacuum chamber with base dimensions of 80 cm $\times$ 160 cm. The system was not optimized for minimum size. The laser cavity with the XUV light generation and extraction stages inside the chamber occupies less than half of the baseplate, so that the footprint of the system could be significantly reduced. Fig. 3 shows pictures of the vacuum chamber with the cavity optical components inside. A scheme of the experimental setup is displayed in Fig. 4. The vacuum chamber is evacuated to a pressure of $\sim 10^{-4}$ mbar with two turbomolecular pumps (HiPace 700 and HiPace 300 from Pfeiffer Vacuum). The turbomolecular pumps are not mechanically isolated from the vacuum chamber but directly attached to it with standard ISO-K flanges. The laser is built on a breadboard, which is fixed to the vacuum chamber baseplate in four points.

The gain element is a wedged 200-µm-thick $Yb:Lu_2O_3$ disk contacted on a water-cooled diamond heat-sink. $Yb:Lu_2O_3$ gain medium was chosen instead of the commonly used Yb:YAG due to its higher thermal conductivity and 30 % larger emission bandwidth [107], which is beneficial for shorter pulse generation in SESAM-mode-locked oscillators [80]. The thin disk is pumped

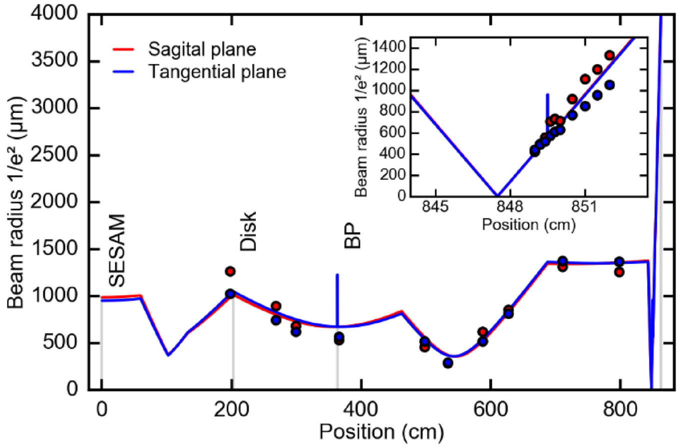

Fig. 5. Intracavity beam radius in the sagittal (red) and tangential (blue) planes in the TDL oscillator. The inset shows a zoom of the beam evolution around the tight focus. The circles show the experimentally assessed beam size and the lines result from numerical cavity simulations.

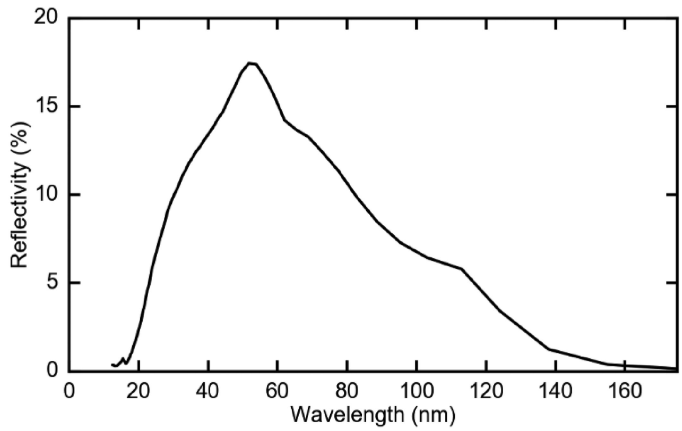

Fig. 6. Theoretical reflectivity of sapphire for p-polarized XUV light when placed at Brewster's angle for 1034-nm infrared light. Data from [111].

by a fiber-coupled laser diode module wavelength-stabilized by a volume-Bragg-grating (VBG) at the 976-nm zero-photon line, allowing for laser operation with low quantum defect. The thin disk is used as a folding mirror in the standing-wave cavity.

A SESAM inserted as an end mirror initiates the mode-locking operation. It is made of four InGaAs quantum wells (QWs), placed in two pairs in subsequent antinodes of the electric field. An embedment of the QWs in AlAsP layers ensures full strain compensation of the epitaxial structure [108]. A dielectric top-coating is added to reduce the field enhancement and prevents negative effects related to multi-photon absorption [109]. The SESAM has a modulation depth of 1.6 %, nonsaturable losses of 0.3 % and a saturation fluence of 47.5 µJ/cm^2. The beam radius on the SESAM and on the disk was estimated to 0.95 mm and 1.15 mm, respectively. These values were obtained by measuring the radius of ten beams leaking out of the cavity through flat folding mirrors at various locations in the resonator. The beam size inside the cavity was deduced from these measurements by considering a Gaussian beam propagation. The obtained results show a fair agreement with numerically simulated values (see Fig. 5). A 4-mm-thick undoped YAG plate is placed at Brewster's angle to enforce the linear p-polarization and introduce enough SPM for soliton mode-locking. The SPM is balanced by three dispersive mirrors that introduce a total intracavity group delay dispersion of -3000 fs^2 per roundtrip. An output coupler with a transmission of 0.7 % is used as a folding mirror.

D. Tight-Focus Extension

To reach sufficient peak intensity for the HHG process, a cavity extension containing a tight intracavity focus was implemented. Cavity simulations showed that a strong astigmatism is induced when using highly focusing mirrors even with an angle of incidence of a few degrees only. This astigmatism can potentially be an issue for the overlap of the pump beam with the laser mode on the thin disk and, thus, for the stability of the entire system. Therefore, the second curved mirror after the tight focus is set as an end mirror and a tight intracavity focus occurs between the two curved mirrors with a radius of curvature of 100 mm and 150 mm, respectively (the latter one being used as a cavity end mirror). A critical challenge for the intra-oscillator HHG system is the careful determination of the focus size. Indeed, HHG being an extreme nonlinear process, a small error of 10 % in the estimation of the focal size can easily lead to an order of magnitude difference in the dipole response and strongly affect the whole process. To properly measure the beam waist at the focus, a 250-µm-thin wedged sapphire plate was placed in the cavity before the tight focus position. The profile of the beam reflected by the sapphire plate was measured over the course of its propagation. Taking into account the measured $M^2_{x,y} < 1.02$, a beam radius of $\sim$12 µm was determined at the focus (see Fig. 5, inset). This value is in fair agreement with the calculated intracavity beam size according to the simulations presented in Fig. 5. In the future, additional methods can be used to estimate the laser beam size at the interaction point. The method recently proposed by Comby and co-authors [110] allows for the determination of the absolute density profile of a gas jet used for HHG by measuring the brightness profile of the generated plasma. As an intermediate step, the authors disentangled the contributions of the laser beam profile evolution from the gas jet itself by measuring the profile of the created plasma with a constant argon pressure in the chamber. This method may find application for laser beam calibrations in intra-oscillator-based HHG systems as well as in systems relying on fsEC.

E. Extraction of the XUV Light

Similarly to HHG driven by fsEC, the extraction of the generated XUV light from the optical cavity needs to have a low impact on the driving laser while being efficient for the XUV light. As mentioned in the introduction, several methods have been developed for fsEC. For the described proof-of-principle demonstration of intra-oscillator HHG, a wedged sapphire plate with a thickness of 250 µm was placed at Brewster's angle for the laser wavelength, 2 cm behind the focus.

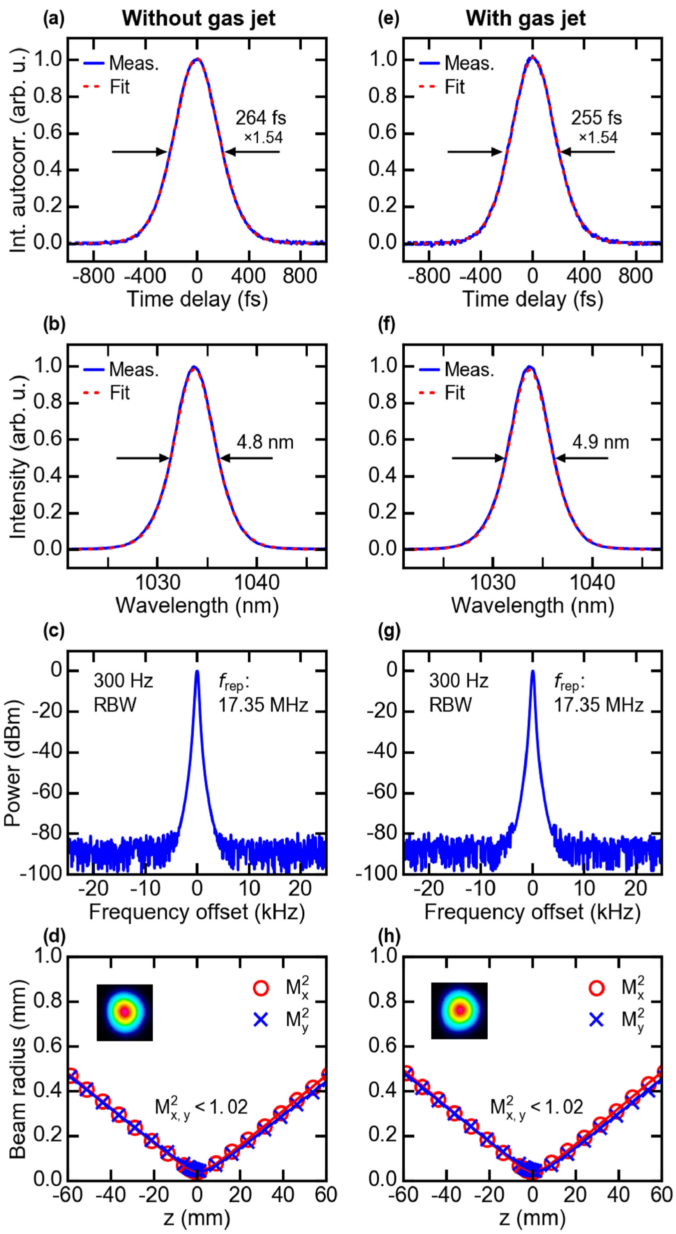

Fig. 7. Comparison of the TDL oscillator parameters without high-pressure gas jet (a-d), and with high-pressure gas jet during the HHG process (e-h). Intensity autocorrelation traces (a, e), optical spectra (b, f), RF spectra (c, g), and M^2 factor measurements (d, h). Insets in (d, h) show the output beam profile. Adapted with permission from [49].

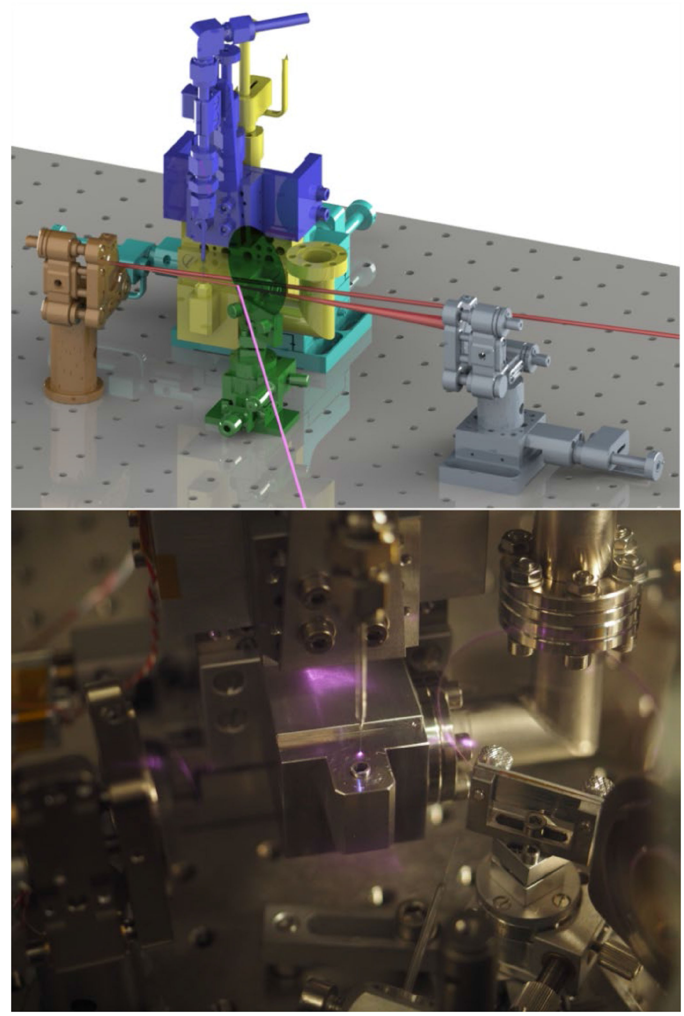

Fig. 8. CAD view of the XUV generation setup (top). The x-y axes translation stage moving both the nozzle and the gas jet dump is displayed in cyan, the nozzle and its vertical translation stage in blue, the gas jet dump and its vertical translation stage in yellow, the first CM in brown, the second CM in grey, the sapphire plate and its holder in green. Picture of the interaction point during the HHG process (bottom).

While its reflection is negligible at the laser wavelength, the refractive index difference between the infrared and XUV light beams allows for a reflection of 7 % at $\lambda = 100$ nm and up to 15 % at $\lambda = 60$ nm (see Fig. 6 showing the theoretical reflectivity in the XUV region of a sapphire plate placed at Brewster's angle for the infrared light at 1034 nm).

F. Laser Performance Without HHG

Without the gas target, the laser generates 264-fs pulses at a repetition rate of 17.35 MHz with an intracavity average power of 320 W at a pump power of 49 W. The intracavity peak power of 62 MW leads to a peak intensity of $\sim 2.7 \times 10^{13}$ W/cm^2 at the focus. The corresponding properties of the laser are shown in Fig. 7(a-d). At higher pump power levels without HHG process, the authors observed mode-locking instabilities, most likely arising from operation close to the roll-over of the SESAM reflectivity in combination with the finite bandwidth of the gain material [80], [112]. Those limitations will be discussed in further details in Section III-B.

G. XUV Generation

A quartz nozzle with ~100–µm opening diameter is used for gas delivery into the tight focus. In order to keep the chamber pressure below 5×10^{-3} mbar while a high-pressure gas jet is used, a gas jet dump is placed below the nozzle and is connected to a primary pump [113]. A computer-aided design (CAD) view and a picture of the XUV generation section are shown in Fig. 8. Since the HHG signal is very dependent on the nozzle position (see, e.g., [114]–[116]), the gas delivery system with the dump

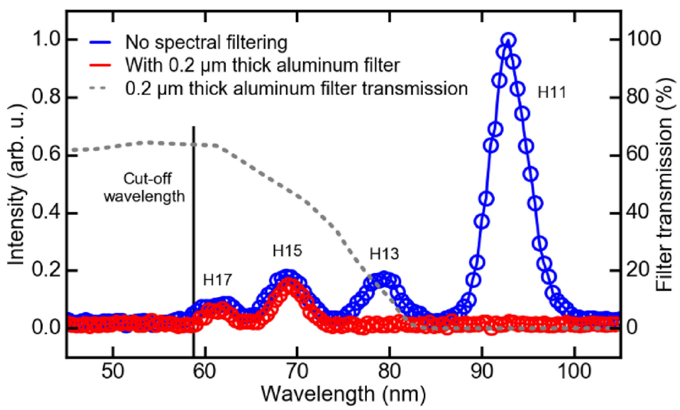

Fig. 9. Measured spectra of the generated XUV light (with a spectral resolution of 3.4 nm). The full spectrum is plotted in blue while the spectrum filtered by a 0.2-µm-thick aluminum foil is plotted in red. The theoretical transmission of the aluminum filter is shown for reference and plotted as grey dashed line (right vertical axis). Adapted with permission from [49].

is installed on a translation stage. Both the quartz nozzle and the gas jet dump are mounted on translation stages to precisely adjust their position along and across the laser beam. The vertical position of the gas jet dump is set during the cw laser operation to ensure that no clipping of the laser beam occurs. The position of the gas nozzle is adjusted independently for the maximum detected XUV signal during the mode-locked laser operation with HHG. A quartz nozzle was chosen instead of a metallic one to avoid a possible contamination of the mirrors and of the vacuum chamber in the case of a nozzle damage by laser pulses.

H. Detection of the XUV Light

The authors use 3.4 bar of xenon backing pressure in the quartz nozzle, which leads to a pressure at the laser focus estimated to 400 mbar. At this gas pressure, the average output power of the laser slightly decreased by a few percent and the pump power was increased from 49 W to 51 W to retrieve the same intracavity average power of 320 W as without gas jet. The TDL oscillator with HHG operates with slightly shorter pulses of 255 fs and its intracavity peak power of 64 MW leads to a peak intensity of $\sim 2.8 \times 10^{13}$ W/cm^2 at the tight focus. The corresponding properties of the laser are shown in Fig. 7(e-h). By comparing the TDL oscillator parameters with and without the high-pressure gas jet, and especially the RF signal and the transverse beam quality, one notices that the HHG process has a negligible influence on the laser performance.

High harmonics up to the 17th order (60.8 nm, 20.4 eV) were detected, in accordance with predictions from the cut-off formula [117]. The recorded XUV spectrum is shown in Fig. 9. Harmonics below the 11th order (94 nm, 13.2 eV) were not detected, most likely due to reabsorption in xenon for the 9th harmonic (114.9 nm, 10.8 eV) [46] and the low quantum efficiency of the detector in the spectral range corresponding to the 7th harmonic (147.7 nm, 8.4 eV) and at longer wavelengths. A second spectrum was acquired after placing a 0.2-µm-thick aluminum filter before the monochromator. Aluminum has a sharp drop in transmission at wavelengths above 70 nm (see Fig. 9). Therefore, the 11th and 13th harmonics (respectively at 94 nm and 79.5 nm) are suppressed in this additional measurement, which confirms that the two highest detected harmonics are H15 and H17) A very conservative estimation results in a generated flux of $\gtrsim 2.6 \times 10^8$ photons/s in the 11th harmonic. This corresponds to an average power $\gtrsim 0.55$ nW and a conversion efficiency $\gtrsim 1.7 \times 10^{-12}$ with respect to the intracavity average power and $\gtrsim 1.1 \times 10^{-11}$ with respect to the pump power. Details on the detection system can be found in [49].

III. Towards a High-Flux XUV Light Source via Intra-Oscillator HHG With TDLs

While the achieved flux for the first reported intra-oscillator HHG systems was lower than state-of-the-art XUV light sources at megahertz repetition rates, this does not seem to be a fundamental limitation. It is important to note that other approaches of HHG at megahertz repetition rates delivered similar values in their first reported implementation. The key challenge is to assess if the XUV flux obtained by the intra-TDL HHG is scalable and whether it is capable of reaching similar or higher XUV fluxes than other approaches at megahertz repetition rates.

In this section, we discuss a roadmap towards a high-flux table-top XUV light source based on intra-oscillator HHG with TDLs. We first present a short review of the relevant parameters for high-flux XUV sources based on HHG. Then we summarize the highest XUV light fluxes reported at megahertz repetition rates and the corresponding parameters of the driving laser. From this inventory, we compare state-of-the-art performance achieved with TDL oscillators with other laser systems used for XUV generation, and show the promising potential of the TDL oscillator technology for high XUV flux sources based on HHG. Finally, we compare study a potential efficient scheme for the extraction of the XUV light.

A. Requirements for an Efficient HHG Process

Since its discovery three decades ago [8], [9], the HHG process in noble gases has been intensively studied, and the response of a single atom during the process is now well understood [118], [119]. Therefore, it is not the topic of this review paper to explain it and we refer the reader to the previously cited articles for more detailed explanations. However, it is important to understand some basic scaling laws in order to identify the important parameters to develop a high XUV flux source based on intra-oscillator HHG.

Based on the formalism introduced by Heyl and co-authors [120], the number of emitted photons at a given harmonic order q scales as $S_q \propto A_q^2 S_{\Delta\phi}$ where A_q is the amplitude of the atomic response for the qth harmonic and $S_{\Delta\phi}$ is a function that includes macroscopic effects such as the phase-matching of the emitted XUV light. Whereas A_q can be calculated from quantum mechanics [118], an empirical formula has been derived, resulting in a scaling law for this quantity when the laser peak intensity I_{peak} is above the cut-off intensity $I_{\mathrm{cut-off},q}$, which corresponds to harmonics in the plateau region [121]. This empirical formula leads to $S_q \propto (I_{\mathrm{peak}}/I_{\mathrm{cut-off},q})^{9.2} S_{\Delta\phi}$. It clearly shows that for a given harmonic order, a small increase in the laser peak intensity can potentially lead to a large increase in the number

TABLE I

SELECTION OF DRIVING SOURCE PARAMETERS OF HHG-BASED XUV SOURCES WITH REPETITION RATES ABOVE 1 MHz AND CORRESPONDING GENERATED XUV AVERAGE POWER IN A HARMONIC. INTRACAVITY PARAMETERS OF STATE-OF-THE-ART TDL OSCILLATORS (WITH CORRESPONDING GAIN MATERIAL) ARE SHOWN FOR COMPARISON

Driving method	Average power (kW)	Peak power (MW)	Pulse duration (fs)	Peak intensity in the tight focus, if any ($\times 10^{13}$ W/cm^2)	Highest generated XUV average power in a harmonic (corresponding wavelength), if any	Highest generated photon energy, if any (eV)	Reference
fsEC	0.6	132	80	3.7	1.01 mW (113 nm)	23.4	[43]
fsEC	0.6	132	80	3.7	0.72 mW (88 nm)	23.4	[43]
fsEC	3	594	57	9.5	36.6 μW (38.6 nm)	58.3	[45]
fsEC	3.4	673	57	29.8	13.6 pW (12.6 nm)	107.9	[45]
fsEC	10	1170	30	30	72 μW (61 nm)	104.2	[47]
fsEC	2.34	238	120	5	1.9 mW (97 nm)	Not reported	[50]
fsEC	2.34	238	120	5	0.87 mW (63 nm)	Not reported	[50]
CC-FCPA	0.076	140	31	7.4	51.1 μW (45 nm)	31.5	[41]
TDL (Yb:LuO)	0.32	64	255	2.8	0.55 nW (94 nm)	20.4	[49]
TDL (Yb:YAG)	1.12	519	610	8.4	Not reported	51.7	[105]
TDL (Yb:LuO)	0.178	73.3	35	-	-	-	[98]
TDL (Yb:YAG)	1	416	140	-	-	-	[57]
TDL (Yb:YAG)	2.98	1760	520	-	-	-	[78]

of emitted XUV photons. However, an increase of the peak intensity while keeping all other parameters (repetition rate, pulse duration, gas pressure, etc.) constant strongly increases the ionization fraction. This in turns strongly influences the phase matching [13], [122], which is one of the key elements for the final efficiency of the process [123]. Luckily, the phase matching can be improved by tuning the gas pressure to be in the so-called pressure-induced phase matching regime [121]. However, this requires the ionization fraction η to be below a critical value η_{crit} [120], [124]. Furthermore, even if $\eta < \eta_{\mathrm{crit}}$, increasing the ionization fraction leads to an increase of the phase matching pressure as reported in one of the studies presented by Heyl and co-authors [120]. Therefore, increasing only the intracavity peak power while keeping all other laser parameters constant is not necessarily the most efficient approach. It increases the amplitude of the atomic response, but also increases the ionization fraction, potentially leading to $\eta > \eta_{\mathrm{crit}}$ and preventing phase matching. Even in the case where $\eta < \eta_{\mathrm{crit}}$, the phase matching pressure can potentially be so high that it can be impractical to reach, e.g., since turbomolecular pumps might not be able to handle the gas load. However, it was theoretically shown that the peak intensity can increase while keeping the same ionization fraction when the pulse duration is decreased accordingly [124]. Therefore, decreasing the pulse duration while all other parameters remain constant has a strong effect on the phase matching, leading to an increase in the achievable XUV flux as reported, e.g., in [124]. As an example, the authors showed that decreasing the pulse duration from 500 fs to 30 fs could potentially lead to a gain by three orders of magnitude in the XUV flux for the studied 25th harmonic. Therefore, the optimization of the pulse duration is also important to be able to reach the phase-matching pressure at high peak intensities. In conclusion, the first demonstration of intra-TDL oscillator HHG mostly lacked the short pulses duration, but also the intracavity peak power. As seen in Table I, this is also clear when one compares it with state-of-the-art XUV sources based on HHG at megahertz repetition rates. HHG in fsEC resulted in record high XUV average powers, which were obtained at 237-MW intracavity peak power in 120-fs pulses [50]. Therefore, a TDL oscillator achieving intracavity peak powers above 250 MW in sub-100-fs pulses would be a promising candidate for a high-flux XUV generation. As such, it is important to study how the TDL oscillator technology stands today compared to those parameters.

B. SESAM-Mode-Locked TDLs for Intra-Oscillator HHG

The first mode-locked TDL oscillator demonstrated in 2000 [54] employed SESAM mode-locking. This method is simple to implement, because the cavity can be optimized in cw operation, and afterwards one end mirror is simply replaced by a SESAM. This is a significant advantage for realizing complex cavities, such as required for intra-oscillator HHG. On the other hand, for KLM TDL oscillators, the mode-locking regime changes the beam size in the cavity. Therefore, the use of SESAM-mode-locked TDL oscillators appeared to be an easier approach for a first proof-of-principle demonstration of intra-oscillator HHG.

As discussed before, the main requirements on the driving laser for efficient XUV generation via HHG are the laser peak power and pulse duration. In principle, the TDL technology is power scalable [75], [76]. However, for mode-locking operation, other considerations than the scalability of the average power in cw operation have to be taken into account.

The peak-power scalability of SESAM-mode-locked TDL oscillators based on Yb:Lu_2O_3 has been recently addressed [80]. The authors demonstrated a high-peak power SESAM-mode-locked TDL oscillator based on Yb:Lu_2O_3 delivering up to 147.4 MW of intracavity peak power with 616-fs pulses and 35 MW of intracavity peak power in 268-fs pulses. Both results are on the edge of the mode-locking stability and the SESAM operated close to the roll-over region [54].

The authors demonstrated that the roll-over in the SESAM reflectivity induced by two photons absorption (TPA) for short pulses [125] combined with the finite bandwidth of the gain material lead to a reduction in the gain difference between cw and mode-locked operations. For ultra-short pulses, this can ultimately favor cw-breakthrough or double-pulsing operation

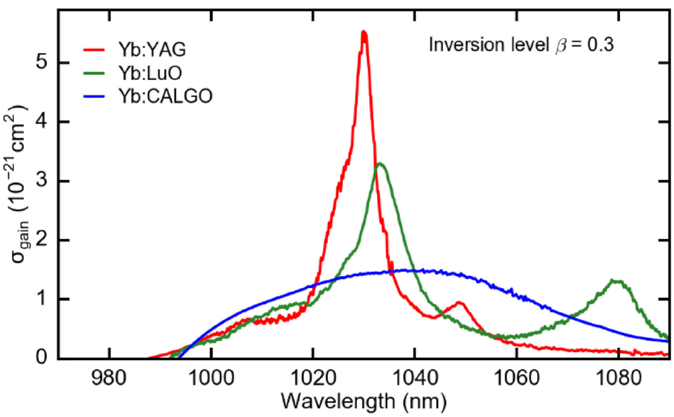

Fig. 10. Gain cross section of Yb-doped YAG, LuO, and CALGO (σ-polarization) calculated for an inversion level $\beta = 0.3$. Data from [107], [126].

[80]. Additionally, TPA leads to an increase in absorption losses that can result in an enhanced thermal lensing via increased heat load and ultimately to a damage of the SESAM due to the heating of the lattice [109]. Gain materials with larger emission and gain bandwidths, such as Yb:CALGO shown in Fig. 10, could allow for a mitigation of the gain reduction between cw and mode-locked operation. However, while this gain material achieved the shortest pulses from TDL oscillators for both SESAM-mode-locked [90] and KLM [81] operation, sub-150-fs Yb:CALGO-based TDL oscillators have not shown intracavity peak power above a few tens of megawatts.

Finally, based on their experimental and numerical results, the authors discussed design guidelines for the realization of a SESAM-mode-locked Yb:LuO TDL oscillator operating with 590 MW of intracavity peak power and 200-fs pulses. They concluded that this will require a beam radius on the SESAM of 2.6 mm to reduce TPA, which is an additional constraint on the cavity design and on the alignment sensitivity of the resonator. Additionally, the gain reduction from the finite gain bandwidth should be balanced by using a SESAM with 10% modulation depth. This would require the growth of strain-compensated structures with more than eight QWs, which can lead to increased losses and, therefore, potentially stronger thermal lensing. However, novel substrate-transferred directly-bonded SESAMs demonstrated reduced thermal lensing under thermal load, very low imperfection and large cold surface flatness [127], which should allow for high intracavity power TDL oscillators with ultrashort pulses. Additionally, novel designs allowing the growth of strain-compensated SESAMs with multiple QWs by metal-organic vapor phase epitaxy [108] can lead in the future to industrial-grade SESAMs suitable for intra-oscillator HHG. Finally, as shown in Fig. 2, there are still very few SESAM-mode-locked TDL oscillators operating with more than a few tens of megawatts of intracavity peak power with sub-150-fs pulses.

Therefore, while SESAMs are a highly successful technology for real-world lasers [128] and numerous new developments such as multi-gigahertz repetition rate laser oscillators for frequency comb applications [129]–[131], further SESAM development is still needed to reach the performance required for intra-oscillator HHG. Furthermore, such SESAMs will most likely initially not be commercially available and difficult to obtain. Hence, at the present time, SESAM-mode-locked TDL oscillators are not the most promising technology for a high-flux XUV source based on intra-oscillator HHG with TDLs.

C. Kerr-Lens Mode-Locked TDLs for Intra-Oscillator HHG

The first proof-of-principle demonstration of a KLM TDL oscillator was reported in 2011 [88]. Nowadays, such lasers have achieved an intracavity peak power of 1.76 GW [78], which is almost an order of magnitude higher than values obtained with SESAM-mode-locked TDL oscillators [56]. Furthermore, KLM TDL oscillators can generate pulses with durations down to 30 fs, which is the shortest value ever achieved with a mode-locked TDL oscillator [81]. These two results already show that KLM TDL oscillators can achieve sufficiently large intracavity peak power and short pulses duration for efficient HHG. However, while the combination of high intracavity peak power with sub-150-fs pulses is problematic for current SESAM-mode-locked TDL oscillators, those two parameters are not necessary competing with each other in KLM TDL oscillators. A few years ago, Brons and co-authors investigated the peak power scaling of an ultrafast Yb:YAG KLM TDL oscillator [79]. They showed that a linear increase of the beam size in the Kerr medium allows for a linear increase of the maximum achievable intracavity peak power without significant changes of the pulse duration. Applying this scaling procedure, they achieved more than 400 MW of intracavity peak power and 140-fs pulses with an intracavity average power of 1 kW [57]. This work does not only show that the KLM TDL concept is scalable in peak power with minor effect on the pulse duration, but also demonstrates that KLM TDL oscillators can achieve intracavity peak power levels comparable to passive enhancement cavities used for state-of-the-art HHG (see Table I).

While Yb:YAG-based TDL oscillators have shown 49-fs pulses with 35 MW of intracavity peak power [132], the gain material Yb:LuO supports a larger optical bandwidth (see Fig. 10). Operated in the strongly SPM-broadened regime where the optical spectrum exceeded the emission bandwidth, Yb:LuO has already generated 35-fs pulses with 77-MW intracavity peak power while operating in ambient air [98]. Therefore, applying the aforementioned scaling procedure to this TDL oscillator should allow achieving multi-hundreds of MW in sub-50-fs pulses. Furthermore, broadband gain materials such as Yb:CALGO offer even larger emission bandwidths (see Fig. 10). Given the current results for enhancement-cavity-driven HHG, it can reasonably be expected that such laser performance would be suitable for a high-flux XUV light source at megahertz repetition rate. It has also to be noted that a new KLM TDL oscillator based on Ho:YAG gain material has recently been demonstrated [133]. While its current performance are not good enough to efficiently perform HHG, a power scaling of this system can lead to HHG with a higher cut-off energy resulting from the longer laser emission wavelength centred at 2 µm. Furthermore, mode-locking of a TDL oscillator with the frequency-doubling nonlinear-mirror technique has been achieved [134] and could be a promising alternative in the future. Finally, it is important to note that for most of the results discussed here, the ultrafast TDL oscillators were optimized for output and not for intracavity parameters. This leaves room for further performance improvements for both SESAM and KLM TDL oscillators towards better driving source for intracavity HHG.

D. Nonlinear Plasma Effects

As it was discussed in the previous section, reaching sufficiently high intracavity peak powers combined with short pulse duration to efficiently drive HHG is well within reach of the TDL oscillator technology. An important question is if strong plasma effects may prevent stable mode-locking operation of the laser oscillator. The proof of principle demonstration described earlier was realized at relatively low peak intensity and low ionization levels.

As mentioned in the introduction, plasma-induced nonlinearities strongly affect fsEC. As such, significant work has been done to understand these processes and to mitigate their negative effects. Already in 2005, Moll and co-authors investigated numerically the effect of χ^3 nonlinearities in fsEC and highlighted a reduction of the enhancement factor arising from the nonlinear phase shift experienced by the pulse inside the cavity nonlinear medium [135]. It was found that an approximate value for this nonlinear phase shift was $\approx \pi/F$ where F is the finesse of the fsEC. The first experimental studies of plasma induced nonlinear dynamics in fsEC were done in 2011 by Carlson and co-authors [70] and Allison and co-authors [71]. Later on, another study by Holzberger and co-authors [72] demonstrated that this value was almost twice higher $\approx 6.3/F$.

In the literature for state-of-the-art fsEC driven HHG, the finesse is generally not stated but only the enhancement factor. Estimating the lowest finesse at which the stated enhancement can be reached allows to calculate an upper value for the maximum tolerable nonlinear phase-shift. For the previously discussed fsEC state-of-the-art results, this leads to a nonlinear phase shift in the order of 10 mrad to 20 mrad. These values are very low compared to the limits at which mode-locked laser oscillators can stably operate. For example, in the SESAM-mode-locked TDL oscillator reported in Section II, the estimated nonlinear phase shift was $\sim$140 mrad which is already an order of magnitude higher. Furthermore, in KLM TDL oscillators, it is not unusual for the soliton to experience a nonlinear phase shift above 1 rad and up to $\sim$5 rad have already been reported [57].

Mitigation strategies developed for fsEC will most likely also be suitable for intra-oscillator HHG. For example, in [50], the authors showed that by using a novel design for the nozzle [136] combined with a mixture of xenon with some lighter atom like helium, the steady state ionization is decreased to negligible levels. In this way, the plasma is removed before a new pulse starts interacting with the gas jet, thus strongly reducing the nonlinear phase shift induced by the steady-state plasma.

Besides the nonlinear phase shift, a second limiting effect arises from spatial inhomogeneity. Due to the strong nonlinearity of the field ionization, the plasma density can be much higher in the central part of the beam than on its edges which leads to wavefront distortion. The plasma then acts as a diverging lens. In fsEC, this has been shown to lead to the coupling of power from the fundamental Gaussian mode to higher order transverse modes [71]. However, this effect was mitigated by decreasing the cavity finesse. For HHG in a mode-locked laser oscillator, the transverse mode-coupling effect should be similar as in fsEC. However, the total cavity losses are significantly higher than in enhancement cavities. In addition, the high order modes are stronger attenuated than the fundamental mode, for example due to the hard aperture KLM process and the mode-matched pump radiation.

Of course, the nonlinear response introduced by HHG is different from the one introduced by a Kerr medium in a TDL oscillator and it is important to perform further experimental and numerical analysis to obtain a better understanding. Nevertheless, given the difference in magnitude between the both technologies, we expect that nonlinear phase effect should not be a limiting factor for intra-oscillator HHG.

E. XUV Light Extraction

Another very important part of a high-flux XUV light source based on intra-oscillator HHG is the efficient extraction of the generated XUV light. Whereas the effect of the extraction on the driving field is usually not important in the common single-pass approach, here it is crucial to minimize its influence. In that way, the intra-oscillator HHG approach is similar to the fsEC and, thus, the challenges and solutions are similar too.

As discussed in the introduction, significant research work has been done in the fsEC community to develop efficient schemes for XUV light extraction. Comparing the different methods, we expect that the holey mirror technology [45], [65] is very well suited for intra-oscillator HHG. This technique uses the divergence property of Gaussian beams, which scales with the wavelength. In the far field, this can lead to a several times smaller beam size for generated XUV light compared to the infrared driving laser one on the cavity mirror placed after the generation point. A small hole is drilled into this mirror, through which the XUV light is transmitted. Due to its larger size on the mirror, the infrared driving light is reflected and only experiences negligible losses. The hole must be small enough to not introduce significant losses to the driving laser field and large enough to allow the XUV light to propagate through with sufficiently low losses. In the first proof of principle, the hole was manufactured by inverse laser drilling, more detail on the procedure can be found in [45], [137]. The radius of the hole clear aperture used for the out-coupling of the XUV light was 40 µm. Shell breaks at the edge of the hole led to an outer radius of 80 µm, which increased the losses on the driving field without increasing the out-coupling efficiency. In a latter publication, sharper edges were obtained with laser drilling in a conventional geometry [47].

An out-coupling efficiency for the qth harmonic was estimated to be $T_q = 1 - \exp[-2(r/w)^2]$, where r is the hole radius and w the beam radius of the qth harmonic on the mirror [45]. A strong benefit of this geometrical method is its broadband XUV transmission and the fact that the efficiency increases for higher out-coupled photon energy. In [45], the authors calculated the theoretical transmission of the XUV light in a typical fsEC system, which ranges from ∼6.4% at around 60 nm to ∼92% at 10 nm. Using the authors' data, one can calculate that the losses induced to the fundamental beam were below 1%. Taking the same geometry as in [45], a hole with a 80-μm radius would increase the transmission of the XUV light to 23.4% at $\lambda = 60$ nm and to 100% at $\lambda = 10$ nm. Using a worst case scenario where the shell breaks would increase by the same proportion and lead to a 160-μm outer radius, the losses induced on the fundamental beam would amount to 3.46%. While such losses might not be suitable for fsEC since they would strongly reduce the enhancement factor, they can be easily tolerated in a TDL oscillator. In the system presented in [49], the total output coupling of the infrared light is 1.4%. It even amounted to 15% in the state-of-the-art TDL oscillator [57] that was compared in the previous section to enhancement cavity driving HHG. Thus similar losses will be easily tolerable in future intra-oscillator HHG systems based on TDLs. Therefore, it should be possible to implement an efficient XUV output coupling with a holey mirror approach. However, it has to be noted that Carstens and co-authors developed a more accurate model to predict the XUV beam divergence [47] and concluded that it should be significantly higher than initially predicted by the simplified model reported in [45], which affects the out-coupling efficiency of the XUV light. Furthermore, this method has not been implemented so far in a mode-locked oscillator cavity, and it might influence, e.g., the suppression of higher order transverse modes. Finally, an operation with a spatially-tailored driving field [138] has allowed the use of the output coupling method with a much higher output coupling efficiency while lowering the losses for the fundamental driving field [139]. However, implementation of such higher-order modes inside a mode-locked ultrafast oscillator has yet to be demonstrated.

In conclusion, the holey mirror approach appears to be very well suited for high-flux XUV light sources based intra-oscillator HHG if the target is high photon energies. However, due to its geometrical properties, it might not be suitable as efficient output coupling method for lower photon energies, e.g., in the 100-nm to 50-nm range. There, depending on the application, the AR-coated XUV beamsplitter [68] or the intracavity diffraction grating [38] are promising options too.

IV. Towards XUV Frequency Combs Based on Intra-Oscillator HHG With TDLs

XUV optical frequency combs are very attractive tools for many applications such as spectroscopy of electronic transitions in molecules [140], experimental tests of bound-state and many-body quantum electrodynamics in singly ionized helium and neutral helium [21], [141], [142], or searches for variation of fundamental constants [143] using the enhanced sensitivity of highly charged ions [144]. Future applications in precision measurement with highly charged ions [144], helium [142], or hydrogen-like and helium-like ions [141] necessitate phase-stable light in the XUV. Furthermore, it is also required in future nuclear clocks based on XUV transitions in ^{235}U and ^{229}Th [145]–[150].

A. XUV Frequency Combs

A key challenge in all applications of XUV frequency combs is the available power per line. In order to increase it, an overall high power in the XUV is beneficial as well as high repetition rates. So far, the best results have been obtained by HHG driven by a fsEC [22]. As discussed in Section III, intra-oscillator HHG with TDLs is a promising approach to generate high-flux XUV light. In the following, we discuss CEO stabilization of TDL oscillators and the potential to use them for XUV frequency combs. Powerful optical frequency combs based on TDL oscillators may have other applications such as the generation of mid-infrared frequency combs via nonlinear parametric frequency conversion [156], [157]. For this reason, there has been a significant research effort to develop frequency combs based on that technology since the first demonstration of a self-referenced TDL oscillator [97]. In this section we first review the f_{CEO} stabilization of TDL oscillators. Afterwards, we discuss the challenges of f_{CEO} stabilization of a TDL with an intra-oscillator HHG process and present preliminary results.

B. CEO Frequency Stabilization of TDL Oscillators

A selection of CEO frequency stabilized TDLs with relevant oscillator parameters is listed in Table II. The first f_{CEO}-stabilized SESAM-mode-locked TDL oscillator was based on Yb:CALGO as gain medium. It delivered sub-100-fs pulses at 65-MHz repetition rate, but at intracavity average and peak powers of only 84 W and 12.7 MW, respectively [151]. However, as it was explained in [80], power scaling of SESAM-mode-locked TDL oscillators with sub-150-fs pulses is not straightforward.

The first f_{CEO}-stabilized KLM TDL oscillator was based on Yb:YAG as gain medium [152], [158]. The 250-fs pulses required a nonlinear pulse compression stage in order to get short enough pulses for subsequent coherent supercontinuum generation (SCG) [159]. Both pump current modulation and an intracavity acousto-optic modulator (AOM) were used to control the f_{CEO}. With only direct pump modulation, 250 mrad of residual integrated phase noise was achieved (in-loop, integrated from 1 Hz to 500 kHz). Direct pump current modulation is fairly direct to implement, but the locking bandwidth is limited by the gain lifetime and the cavity dynamics. Although this limitation can be compensated to a certain extend with a phase lead filter, the use of an intracavity AOM resulted in a higher stabilization bandwidth and is not limited by the gain dynamics. As a result, a robust tight lock was achieved with 100-mrad residual integrated phase noise (in-loop, integrated from 1 Hz to 500 kHz), combined with high f_{CEO} stability.

The same research group recently reported the f_{CEO} stabilization of a TDL oscillator with more than 200 MW of intracavity peak power [154]. In this conference submission, the authors proposed a novel approach where the intracavity AOM used for

TABLE II
SELECTION OF CEO FREQUENCY STABILIZED TDL OSCILLATORS BASED ON DIFFERENT GAIN MATERIALS AND MODE-LOCKING PROCESSES WITH RELEVANT PARAMETERS OF THE OSCILLATOR

Gain material	Intracavity average power (W)	Intracavity peak power (MW)	Pulse duration (fs)	Repetition rate (MHz)	Mode-locking process	Non-linear pulse compression	Modulation	Residual phase noise (mrad)	Integrating bandwidth	Reference
Yb:CALGO	84	12.6	90	65	SESAM	No	Pump diode	120	1 Hz-1 MHz	[151]
Yb:YAG	309	25.6	250	40	Kerr-lens	Yes	Pump diode	250	1 Hz-500 kHz	[152]
Yb:YAG	309	25.6	250	40	Kerr-lens	Yes	AOM	100	1 Hz-500 kHz	[152]
Yb:YAG	321	30	250	37.5	Kerr-lens	Yes	Pump diode	390	1 Hz-500 kHz	[153]
Yb:YAG	700	207	190	15.6	Kerr-lens	Yes	AOM	90	1 Hz-500 kHz	[154]
Yb:LuO	163	47	50	61	Kerr-lens	No	Pump diode	197	1 Hz-1 MHz	[155]

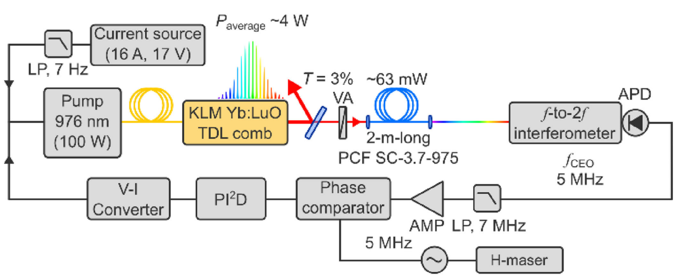

Fig. 11. Schematic of the experimental setup for f_{CEO} detection and stabilization. Electrical connections are indicated by black lines. AMP: amplifier; APD: avalanche photodiode; LP: low-pass filter; P_{average}: average power; PCF: photonic crystal fiber; T: transmission; VA: variable attenuator; V-I converter: voltage-to-current converter; $\mathrm{PI^2D}$: proportional-double-integral-derivative servo controller; ∼: waveform generator. Adapted with permission from [155].

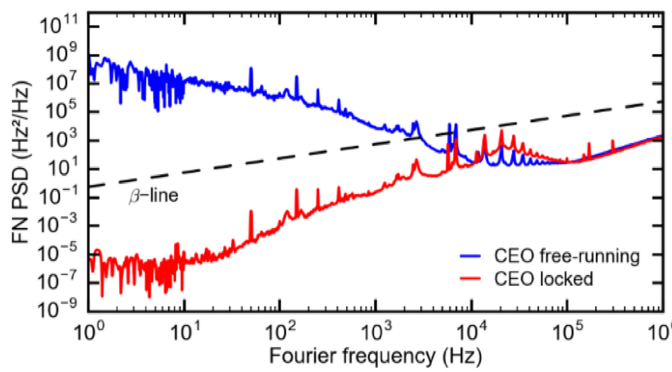

Fig. 12. Frequency noise power spectral density (FN-PSD) of the free-running (blue) and locked (red) CEO beat. The dashed line represents the β-separation line [164]. Adapted with permission from [155].

f_{CEO} stabilization also serves as the Kerr medium for KLM. A residual integrated phase noise of 90 mrad was achieved (in-loop, integrated from 1 Hz to 500 kHz). While the 190-fs long pulses still required an additional nonlinear pulse compression stage prior to the SCG, the high intracavity peak power is already very promising for the development of an XUV optical frequency comb based on intra-oscillator HHG. However, the insertion of such an AOM can be an issue for intracavity HHG with kilowatt average power levels. Thermal effects that can perturb the oscillator and the need to increase the beam size in the AOM may reduce its modulation bandwidth [160]. Nevertheless the reported result was achieved with an average intracavity power of 700 W which is already interesting for intra-oscillator HHG.

Opto-optical modulation (OOM) is another possible method for f_{CEO} stabilization of high-power TDL oscillators. So far, the method has been demonstrated only in DPSSLs [161]–[163], but is also highly promising for TDLs. It is expected to be applicable with kW of intracavity average power and high pulse energies.

As discussed in Section III, operation with sub-150-fs is desirable for intra-oscillator HHG and a promising approach is to operate the TDL oscillator in the strongly SPM-broadened regime. So far, there has been only one study of f_{CEO} stabilization in this regime [155]. The intracavity peak power was already 47 MW and owing to the 50-fs pulse duration, only 63 mW of output power were used for direct SCG, without the need for a nonlinear pulse compression stage [155]. Applying the peak power scaling procedure mentioned in Section III to this TDL oscillator operating in this regime should allow for a powerful driving source for intra-oscillator HHG, which makes this result very promising. Therefore, we give some more details of this system here. The TDL oscillator was previously described in [98] and its parameters are summarized in Table II. The experimental setup for CEO stabilization is shown in Fig. 11. Using feedback to the current of the pump laser diode, a tight phase-lock was achieved. In locked operation the CEO frequency noise power spectral density was strongly reduced up to a bandwidth of 10 kHz as illustrated in Fig. 12. The residual integrated phase noise was 197 mrad (in-loop, integrated from 1 Hz to 1 MHz).

C. CEO-Frequency Stabilization of a TDL Driving an Intra-Oscillator HHG Process

Self-referencing of a TDL oscillator has been done with different techniques and in different conditions as discussed in the previous section. However, it has never been done in combination with an extreme nonlinear process such as HHG occurring inside the oscillator cavity. The previously discussed results on f_{CEO}-stabilized TDL oscillators are highly encouraging for the development of future XUV frequency combs

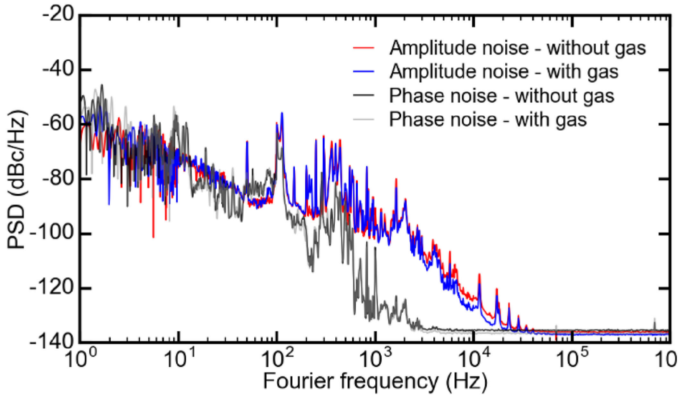

Fig. 13. Amplitude and phase noise of the mode-locked TDL oscillator in free-running operation with and without gas target for HHG. The diagram shows the measurements done on the passively filtered 4th harmonic of the 17.35-MHz repetition rate. Adapted with permission from [49].

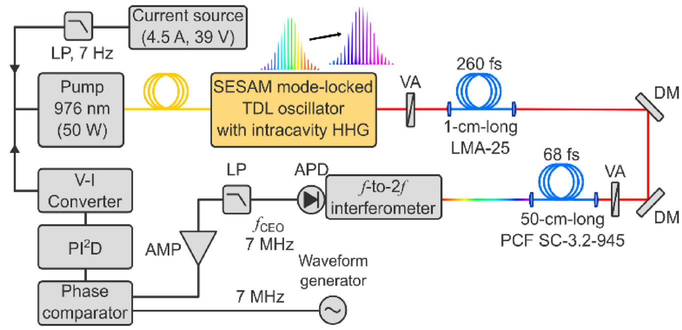

Fig. 14. Scheme of the f_{CEO} detection and stabilization setup. VA: optical attenuator with variable transmission; DM: dispersive mirror; APD: avalanche photodiode; LP: low-pass filter; AMP: signal amplifier; PI^{2}D: proportional-double-integral-derivative servo controller. Black lines represent electrical connections.

TABLE III
NOISE OF THE FREE-RUNNING TDL OSCILLATOR INTEGRATED FROM 1 Hz TO 1 MHz

	Amplitude noise (%)	Phase noise (mrad)
Without gas	0.76	1.25
With HHG	0.78	1.33

based on intra-oscillator HHG. However, there are additional challenges, such as the interaction with the plasma generated during the HHG process [70]–[72] or mechanical noise induced from the vacuum pumping system, which may also affect the performances. Furthermore, stabilization of the repetition rate in combination with f_{CEO} is required to obtain a fully-stabilized optical frequency comb. Whereas some preliminary results have been obtained in that direction [165], it still remains to be done. Additionally, the impact of the HHG process on the laser noise must be analyzed to assess that no significant perturbation is added.

The amplitude and phase noises of the TDL oscillator described Section II was studied in free-running operation with and without HHG process to evaluate if it induced any perturbations, e.g., from the plasma. The measured power spectral density of the amplitude and phase noises is shown in Fig. 13 and the integrated noise values are reported in Table III. Although the vacuum chamber was connected to two turbomolecular pumps and the opto-mechanical components were not optimized for high stability, the integrated relative intensity noise and phase noise are similar to typical values of free-running TDL oscillators [42], [166]. No significant influence of the HHG process was observed. This outcome is already a promising indication of the possibility of f_{CEO}-stabilization of a TDL oscillator with an intracavity HHG process.

Very recently, the first detection and stabilization of the CEO beat was achieved in this system [167], [168]. To achieve a coherent supercontinuum spectrum required for CEO–beat detection in an f-to-$2f$ interferometer, the output pulses of the TDL were compressed from 260 fs to 68 fs in a 1-cm-long fiber (NKT Photonics LMA25) followed by a pair of dispersive mirrors. An octave-spanning coherent supercontinuum spectrum was then generated in a 50-cm-long highly nonlinear PCF (NKT Photonics, SC-3.2-945) and the CEO beat was detected in a standard quasi-common-path f-to-$2f$ interferometer. The experimental setup is shown in Fig. 14. A CEO beat with a signal-to-noise ratio exceeding 25 dB (in a 3-kHz resolution bandwidth) was observed with and without HHG [see inset in Fig. 15(a)]. The measured frequency noise of the free-running CEO was nearly not affected by the highly nonlinear HHG process and by the high-pressure gas jet in the laser cavity. The strong peak at approximately 6 kHz in the noise spectrum and its corresponding harmonics originate from the current driver of the high-power VBG-stabilized pump diode laser. Noise peaks resulting from the turbomolecular pumps occur at around 1 kHz. Implementing a proper mechanical isolation is expected to reduce the impact of mechanical noise, similar to previous results obtained for HHG in passive enhancement cavities. The CEO beat was phase-locked to a reference signal via an active feedback loop to the pump-diode current. Fig. 15(b) shows the frequency noise of the stabilized f_{CEO} signal with and without HHG process. The frequency noise of the stabilized f_{CEO} remains noticeably higher than the β-separation line [164] and corresponds to an integrated phase noise of 23 rad and 12 rad with and without the HHG process, respectively (integrated from 10 Hz to 100 kHz), which implies that a tight lock was not achieved in this preliminary experiment.

Those preliminary results demonstrate that even in the presence of a strongly nonlinear HHG process inside the cavity, the CEO beat of a TDL oscillator can be detected and stabilized via direct pump current modulation. A reduction of the pump diode noise and a better mechanical isolation of the turbomolecular pumps are expected to lower the CEO frequency noise below the β-separation line in the frequency range below 5–10 kHz (corresponds to the modulation bandwidth of the currently used stabilization method) to achieve a tight lock. If these optimizations are not sufficient, the implementation of a wider-bandwidth modulation technique such as an AOM or OOM is possible. In addition, the repetition rate of the TDL needs to be stabilized as well to obtain a fully-stabilized XUV frequency comb.

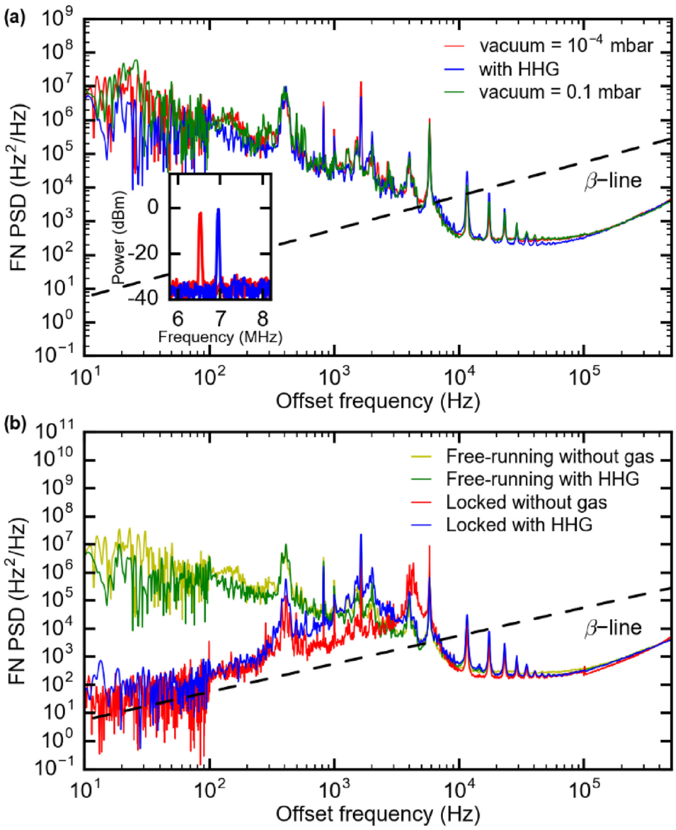

Fig. 15. (a) Frequency noise power spectral density (FN PSD) of the f_{CEO} beat; green: mode-locked laser operated at the pressure of 0.1 mbar, the turbomolecular pumps were off; red: mode-locked laser operated at the pressure of 10^{-4} mbar, the turbomolecular pumps were on; blue: mode-locked laser with HHG in xenon gas jet with estimated gas pressure at the focus of $\sim$400 mbar, the turbomolecular pumps were on. The inset shows the RF spectrum of the detected f_{CEO} beat signals (RBW = 3 kHz, signal-to-noise ratio >25 dB); red: mode-locked laser operated at the pressure of 10^{-4} mbar, the turbomolecular pumps were on; blue: the same laser with the HHG. (b) FN PSD of the stabilized f_{CEO}; red mode-locked laser without HHG; blue: mode-locked laser with intracavity HHG; yellow and green lines represent for a comparison the FN PSD of the free-running f_{CEO} without and with HHG, respectively.

V. Conclusion

As stated in the beginning of this review article, XUV sources operating at megahertz repetition rates have the potential to revolutionize many scientific and technical areas. While the first demonstrations of intra-oscillator HHG with TDLs have so far been strongly limited in performance, a deeper analysis shows that this concept has the potential to reach state-of-the-art XUV performance within the next few years.

As discussed in Section III, KLM TDL oscillators constitute the most promising driving source approach. We expect that the first improvement towards higher XUV fluxes will be relatively easy to implement, following the results obtained from HHG in enhancement cavities. Operated in the strong SPM broadening regime, ultrafast TDL oscillators should be able to deliver intracavity peak power of 300 MW with sub-100-fs pulses, which would only correspond to an improvement of a factor of 4 for the intracavity peak power of the 35-fs Yb:LuO TDL oscillator [98], or of a pulse duration reduction by a factor 0.7 for the 400 MW Yb:YAG TDL oscillator [57] (see Table II). At this performance, an XUV power at milliwatt level generated in the 100-nm to 60-nm region and tens of microwatts at higher photon energies can be expected, if a state-of-the-art gas delivery system is implemented to improve the phase matching of the HHG process [136]. Additionally, the strong research effort that has already been made towards efficient and broadband XUV light output coupler for enhancement cavities could be used for the intra-oscillator HHG concept.

Furthermore, potential applications for XUV frequency combs have been increasing and their development has been so far mainly in the area of enhancement cavities. With the latest developments on optical frequency combs generated from TDL oscillators, those could be an alternative approach for XUV frequency combs. Finally, future development of KLM TDL oscillators in the strongly SPM-broadened regime using gain material with broader emission bandwidths such as Yb:CALGO could lead to sub-20-fs pulses. Combined with gigawatt of intracavity peak power, this should be very beneficial for HHG and could lead to powerful XUV light sources. Therefore, XUV sources based on intra-oscillator HHG with TDL oscillators have a high potential to play an important role in the future, both in scientific and industrial applications.

References

[1] J. Miao *et al.*, "High resolution 3D X-ray diffraction microscopy," *Phys. Rev. Lett.*, vol. 89, no. 8, Aug. 2002, Art. no. 088303.

[2] W. Chao, B. D. Harteneck, J. A. Liddle, E. H. Anderson, and D. T. Attwood, "Soft X-ray microscopy at a spatial resolution better than 15 nm," *Nature*, vol. 435, no. 7046, pp. 1210–1213, Jun. 2005.

[3] B. J. Hillier, K. S. Christopherson, K. E. Prehoda, D. S. Bredt, and W. A. Lim, "Unexpected modes of PDZ domain scaffolding revealed by structure of nNOS-syntrophin complex," *Science*, vol. 284, no. 5415, pp. 812–815, 1999.

[4] H. Luecke, B. Schobert, H. T. Richter, J. P. Cartailler, J. K. Lanyi, "Structural changes in bacteriorhodopsin during ion transport at 2 angstrom resolution," *Science*, vol. 286, no. 5438, pp. 255–261, Oct. 1999.

[5] R. Neutze, R. Wouts, D. van der Spoel, E. Weckert, and J. Hajdu, "Potential for biomolecular imaging with femtosecond X-ray pulses," *Nature*, vol. 406, no. 6797, pp. 752–757, Aug. 2000.

[6] A. Föhlisch *et al.*, "Direct observation of electron dynamics in the attosecond domain," *Nature*, vol. 436, no. 7049, pp. 373–376, Jul. 2005.

[7] L. Young *et al.*, "Femtosecond electronic response of atoms to ultra-intense X-rays," *Nature*, vol. 466, no. 7302, pp. 56–61, Jul. 2010.

[8] A. McPherson *et al.*, "Studies of multiphoton production of vacuum-ultraviolet radiation in the rare gases," *J. Opt. Soc. Amer. B*, vol. 4, no. 4, pp. 595–601, 1987.

[9] M. Ferray *et al.*, "Multiple-harmonic conversion of 1064 nm radiation in rare gases," *J. Phys. B, At., Mol. Opt. Phys.*, vol. 21, pp. L31–L35, 1988.

[10] R. A. Bartels *et al.*, "Generation of spatially coherent light at extreme ultraviolet wavelengths," *Science*, vol. 297, no. 5580, pp. 376–378, Jul. 2002.

[11] C. Benko *et al.*, "Extreme ultraviolet radiation with coherence time greater than 1 s," *Nature Photon.*, vol. 8, no. 7, pp. 530–536, Jun. 2014.

[12] A. Rundquist *et al.*, "Phase-matched generation of coherent soft X-rays," *Science*, vol. 280, no. 5368, pp. 1412–1415, 1998.

[13] T. Popmintchev, M.-C. Chen, P. Arpin, M. M. Murnane, and H. C. Kapteyn, "The attosecond nonlinear optics of bright coherent X-ray generation," *Nature Photon.*, vol. 4, no. 12, pp. 822–832, Dec. 2010.

[14] T. Popmintchev *et al.*, "Bright coherent ultrahigh harmonics in the keV X-ray regime from mid-infrared femtosecond lasers," *Science*, vol. 336, no. 6086, pp. 1287–1291, Jun. 2012.

[15] P. M. Paul *et al.*, "Observation of a train of attosecond pulses from high harmonic generation," *Science*, vol. 292, no. 5522, pp. 1689–1692, Jun. 2001.

[16] M. Hentschel *et al.*, "Attosecond metrology," *Nature*, vol. 414, pp. 509–513, Nov. 2001.

[17] Y. Mairesse *et al.*, "Attosecond synchronization of high-harmonic soft X-rays," *Science*, vol. 302, no. 5650, pp. 1540–1543, Nov. 2003.

[18] C. Hernández-García *et al.*, "Zeptosecond high harmonic keV X-ray waveforms driven by mid infrared laser pulses," *Phys. Rev. Lett.*, vol. 111, no. 3, Jul. 2013, Art. no. 033002.

[19] H. J. Wörner, J. B. Bertrand, D. V. Kartashov, P. B. Corkum, and D. M. Villeneuve, "Following a chemical reaction using high-harmonic interferometry," *Nature*, vol. 466, no. 7306, pp. 604–607, Jul. 2010.

[20] H. J. Wörner *et al.*, "Conical intersection dynamics in NO_2 probed by homodyne high-harmonic spectroscopy," *Science*, vol. 334, no. 6053, pp. 208–212, Oct. 2011.

[21] D. Z. Kandula, C. Gohle, T. J. Pinkert, W. Ubachs, and K. S. E. Eikema, "Extreme ultraviolet frequency comb metrology," *Phys. Rev. Lett.*, vol. 105, no. 6, Aug. 2010, Art. no. 063001.

[22] A. Cingöz *et al.*, "Direct frequency comb spectroscopy in the extreme ultraviolet," *Nature*, vol. 482, no. 7383, pp. 68–71, Feb. 2012.

[23] M. Drescher *et al.*, "Time-resolved atomic inner-shell spectroscopy," *Nature*, vol. 419, no. 6909, pp. 803–807, Oct. 2002.

[24] M. I. Stockman, M. F. Kling, U. Kleineberg, and F. Krausz, "Attosecond nanoplasmonic-field microscope," *Nature Photon.*, vol. 1, no. 9, pp. 539–544, Sep. 2007.

[25] M. Lucchini *et al.*, "Attosecond dynamical Franz-Keldysh effect in polycrystalline diamond," *Science*, vol. 353, no. 6302, pp. 916–919, Aug. 2016.

[26] S. Backus, C. G. Durfee, M. M. Murnane, and H. C. Kapteyn, "High power ultrafast lasers," *Rev. Sci. Instrum.*, vol. 69, no. 3, pp. 1207–1223, Mar. 1998.

[27] R. Dörner *et al.*, "Cold target recoil ion momentum spectroscopy: A 'momentum microscope' to view atomic collision dynamics," *Phys. Rep.*, vol. 330, no. 2/3, pp. 95–192, Jun. 2000.

[28] M. Sabbar *et al.*, "Combining attosecond XUV pulses with coincidence spectroscopy," *Rev. Sci. Instrum.*, vol. 85, no. 10, 2014, Art. no. 103113.

[29] C.-T. Chiang, A. Blättermann, M. Huth, J. Kirschner, and W. Widdra, "High-order harmonic generation at 4 MHz as a light source for time-of-flight photoemission spectroscopy," *Appl. Phys. Lett.*, vol. 101, no. 7, Aug. 2012, Art. no. 071116.

[30] B. Frietsch *et al.*, "A high-order harmonic generation apparatus for time- and angle-resolved photoelectron spectroscopy," *Rev. Sci. Instrum.*, vol. 84, no. 7, 2013, Art. no. 075106.

[31] R. Wallauer, J. Reimann, N. Armbrust, J. Güdde, and U. Höfer, "Intervalley scattering in MoS_2 imaged by two-photon photoemission with a high-harmonic probe," *Appl. Phys. Lett.*, vol. 109, no. 16, Oct. 2016, Art. no. 162102.

[32] C. Corder *et al.*, "Ultrafast extreme ultraviolet photoemission without space charge," *Struct. Dyn.*, vol. 5, no. 5, Sep. 2018, Art. no. 054301.

[33] T. Südmeyer *et al.*, "Femtosecond laser oscillators for high-field science," *Nature Photon.*, vol. 2, no. 10, pp. 599–604, Oct. 2008.

[34] R. Klas *et al.*, "Table-top milliwatt-class extreme ultraviolet high harmonic light source," *Optica*, vol. 3, no. 11, pp. 1167–1170, Nov. 2016.

[35] M. D. Seaberg *et al.*, "Ultrahigh 22 nm resolution coherent diffractive imaging using a desktop 13 nm high harmonic source," *Opt. Express*, vol. 19, no. 23, pp. 22470–22479, 2011.

[36] G. K. Tadesse *et al.*, "High speed and high resolution table-top nanoscale imaging," *Opt. Lett.*, vol. 41, no. 22, pp. 5170–5173, Nov. 2016.

[37] C. Gohle *et al.*, "A frequency comb in the extreme ultraviolet," *Nature*, vol. 436, no. 7048, pp. 234–237, Jul. 2005.

[38] D. C. Yost, T. R. Schibli, and J. Ye, "Efficient output coupling of intracavity high-harmonic generation," *Opt. Lett.*, vol. 33, no. 10, pp. 1099–1101, May 2008.

[39] J. Boullet *et al.*, "High-order harmonic generation at a megahertz-level repetition rate directly driven by an ytterbium-doped-fiber chirped-pulse amplification system," *Opt. Lett.*, vol. 34, no. 9, pp. 1489–1491, 2009.

[40] A. Vernaleken *et al.*, "Single-pass high-harmonic generation at 20.8 MHz repetition rate," *Opt. Lett.*, vol. 36, no. 17, pp. 3428–3430, 2011.

[41] S. Hädrich *et al.*, "Exploring new avenues in high repetition rate table-top coherent extreme ultraviolet sources," *Light, Sci. Appl.*, vol. 4, no. 8, Aug. 2015, Art. no. e320.

[42] F. Emaury, A. Diebold, C. J. Saraceno, and U. Keller, "Compact extreme ultraviolet source at megahertz pulse repetition rate with a low-noise ultrafast thin-disk laser oscillator," *Optica*, vol. 2, no. 11, pp. 980–984, Nov. 2015.

[43] J. Lee, D. R. Carlson, and R. J. Jones, "Optimizing intracavity high harmonic generation for XUV fs frequency combs," *Opt. Express*, vol. 19, no. 23, pp. 23315–23326, Nov. 2011.

[44] S. Hädrich *et al.*, "Generation of μW level plateau harmonics at high repetition rate," *Opt. Express*, vol. 19, no. 20, pp. 19374–19383, Sep. 2011.

[45] I. Pupeza *et al.*, "Compact high-repetition-rate source of coherent 100 eV radiation," *Nature Photon.*, vol. 7, no. 8, pp. 608–612, Aug. 2013.

[46] A. Ozawa, Z. Zhao, M. Kuwata-Gonokami, and Y. Kobayashi, "High average power coherent vuv generation at 10 MHz repetition frequency by intracavity high harmonic generation," *Opt. Express*, vol. 23, no. 12, pp. 15107–15118, Jun. 2015.

[47] H. Carstens *et al.*, "High-harmonic generation at 250 MHz with photon energies exceeding 100 eV," *Optica*, vol. 3, no. 4, pp. 366–369, Apr. 2016.

[48] A. Ozawa *et al.*, "High harmonic frequency combs for high resolution spectroscopy," *Phys. Rev. Lett.*, vol. 100, no. 25, Jun. 2008, Art. no. 253901.

[49] F. Labaye *et al.*, "Extreme ultraviolet light source at a megahertz repetition rate based on high-harmonic generation inside a mode-locked thin-disk laser oscillator," *Opt. Lett.*, vol. 42, no. 24, pp. 5170–5173, Dec. 2017.

[50] G. Porat *et al.*, "Phase-matched extreme-ultraviolet frequency-comb generation," *Nature Photon.*, vol. 12, no. 7, pp. 387–391, Jul. 2018.

[51] A. Klenke *et al.*, "530 W, 13 mJ, four-channel coherently combined femtosecond fiber chirped-pulse amplification system," *Opt. Lett.*, vol. 38, no. 13, pp. 2283–2285, Jul. 2013.

[52] M. Müller *et al.*, "1 kW 1 mJ eight-channel ultrafast fiber laser," *Opt. Lett.*, vol. 41, no. 15, pp. 3439–3442, Aug. 2016.

[53] P. Russbueldt, T. Mans, J. Weitenberg, H. D. Hoffmann, and R. Poprawe, "Compact diode-pumped 1.1 kW Yb: YAG Innoslab femtosecond amplifier," *Opt. Lett.*, vol. 35, no. 24, pp. 4169–4171, 2010.

[54] J. A. der Au *et al.*, "16.2-W average power from a diode-pumped femtosecond Yb: YAG thin disk laser," *Opt. Lett.*, vol. 25, no. 11, pp. 859–861, 2000.

[55] C. J. Saraceno *et al.*, "275 W average output power from a femtosecond thin disk oscillator operated in a vacuum environment," *Opt. Express*, vol. 20, no. 21, pp. 23535–23541, Oct. 2012.

[56] C. J. Saraceno *et al.*, "Ultrafast thin-disk laser with 80 μJ pulse energy and 242 W of average power," *Opt. Lett.*, vol. 39, no. 1, pp. 9–12, Jan. 2014.

[57] J. Brons *et al.*, "Powerful 100-fs-scale Kerr-lens mode-locked thin-disk oscillator," *Opt. Lett.*, vol. 41, no. 15, pp. 3567–3570, Aug. 2016.

[58] G. K. Tadesse *et al.*, "High resolution XUV Fourier transform holography on a table top," *Sci. Rep.*, vol. 8, no. 1, Dec. 2018, Art. no. 8677.

[59] J. Rothhardt *et al.*, "High-repetition-rate and high-photon-flux 70 eV high-harmonic source for coincidence ion imaging of gas-phase molecules," *Opt. Express*, vol. 24, no. 16, pp. 18133–18147, Aug. 2016.

[60] M. Nisoli, S. De Silvestri, and O. Svelto, "Generation of high energy 10 fs pulses by a new pulse compression technique," *Appl. Phys. Lett.*, vol. 68, no. 20, pp. 2793–2795, May 1996.

[61] F. Emaury *et al.*, "Efficient spectral broadening in the 100-W average power regime using gas-filled kagome HC-PCF and pulse compression," *Opt. Lett.*, vol. 39, no. 24, pp. 6843–6846, Dec. 2014.

[62] R. J. Jones and J. Ye, "Femtosecond pulse amplification by coherent addition in a passive optical cavity," *Opt. Lett.*, vol. 27, no. 20, pp. 1848–1850, 2002.

[63] H. Carstens *et al.*, "Megawatt-scale average-power ultrashort pulses in an enhancement cavity," *Opt. Lett.*, vol. 39, no. 9, pp. 2595–2598, May 2014.

[64] R. J. Jones, K. D. Moll, M. J. Thorpe, and J. Ye, "Phase-coherent frequency combs in the vacuum ultraviolet via high-harmonic generation inside a femtosecond enhancement cavity," *Phys. Rev. Lett.*, vol. 94, no. 19, May 2005, Art. no. 193201.

[65] K. D. Moll, R. J. Jones, and J. Ye, "Output coupling methods for cavity-based high-harmonic generation," *Opt. Express*, vol. 14, no. 18, pp. 8189–8197, Sep. 2006.

[66] J. Wu and H. Zeng, "Cavity-enhanced noncollinear high-harmonic generation for extreme ultraviolet frequency combs," *Opt. Lett.*, vol. 32, no. 22, pp. 3315–3317, Nov. 2007.

[67] A. Ozawa *et al.*, "Non-collinear high harmonic generation: A promising outcoupling method for cavity-assisted XUV generation," *Opt. Express*, vol. 16, no. 9, pp. 6233–6239, Apr. 2008.

[68] O. Pronin *et al.*, "Ultrabroadband efficient intracavity XUV output coupler," *Opt. Express*, vol. 19, no. 11, pp. 10232–10240, May 2011.

[69] I. Pupeza, E. E. Fill, and F. Krausz, "Low-loss VIS/IR-XUV beam splitter for high-power applications," *Opt. Express*, vol. 19, no. 13, pp. 12108–12118, Jun. 2011.

[70] D. R. Carlson, J. Lee, J. Mongelli, E. M. Wright, and R. J. Jones, "Intracavity ionization and pulse formation in femtosecond enhancement cavities," *Opt. Lett.*, vol. 36, no. 15, pp. 2991–2993, 2011.

[71] T. K. Allison, A. Cingöz, D. C. Yost, and J. Ye, "Extreme nonlinear optics in a femtosecond enhancement cavity," *Phys. Rev. Lett.*, vol. 107, no. 18, Oct. 2011, Art. no. 183903.

[72] S. Holzberger *et al.*, "Femtosecond enhancement cavities in the nonlinear regime," *Phys. Rev. Lett.*, vol. 115, no. 2, Jul. 2015, Art. no. 023902.

[73] H. A. Haus, "Mode-locking of lasers," *IEEE J. Sel. Topics Quantum Electron.*, vol. 6, no. 6, pp. 1173–1185, Nov./Dec. 2000.

[74] E. Seres, J. Seres, and C. Spielmann, "Extreme ultraviolet light source based on intracavity high harmonic generation in a mode locked Ti: Sapphire oscillator with 9.4 MHz repetition rate," *Opt. Express*, vol. 20, no. 6, pp. 6185–6190, Mar. 2012.

[75] A. Giesen *et al.*, "Scalable concept for diode-pumped high-power solid-state lasers," *Appl. Phys. B Lasers Opt.*, vol. 58, no. 5, pp. 365–372, 1994.

[76] A. Giesen and J. Speiser, "Fifteen years of work on thin-disk lasers: Results and scaling laws," *IEEE J. Sel. Topics Quantum Electron.*, vol. 13, no. 3, pp. 598–609, May/Jun. 2007.

[77] B. Deppe, G. Huber, C. Kränkel, and J. Küpper, "High-intracavity-power thin-disk laser for the alignment of molecules," *Opt. Express*, vol. 23, no. 22, pp. 28491–28500, Nov. 2015.

[78] N. Kanda *et al.*, "High-pulse-energy Yb: YAG thin disk mode-locked oscillator for intra-cavity high harmonic generation," presented at the Adv. Solid State Lasers Congr., 2013, Paper AF3A.8. [Online]. Available: https://www.osapublishing.org/abstract.cfm?uri=ASSL-2013-AF3A.8

[79] J. Brons *et al.*, "Energy scaling of Kerr-lens mode-locked thin-disk oscillators," *Opt. Lett.*, vol. 39, no. 22, pp. 6442–6445, Nov. 2014.

[80] I. J. Graumann *et al.*, "Peak-power scaling of femtosecond Yb:Lu_2O_3 thin-disk lasers," *Opt. Express*, vol. 25, no. 19, pp. 22519–22536, Sep. 2017.

[81] N. Modsching *et al.*, "Kerr lens mode-locked Yb:CALGO thin-disk laser," *Opt. Lett.*, vol. 43, no. 4, pp. 879–882, Feb. 2018.

[82] F. Brunner *et al.*, "240-fs pulses with 22-W average power from a mode-locked thin-disk Yb:$KY(WO_4)_2$ laser," *Opt. Lett.*, vol. 27, no. 13, pp. 1162–1164, Jul. 2002.

[83] E. Innerhofer *et al.*, "60-W average power in 810-fs pulses from a thin-disk Yb:YAG laser," *Opt. Lett.*, vol. 28, no. 5, pp. 367–369, 2003.

[84] S. V. Marchese, T. Südmeyer, M. Golling, R. Grange, and U. Keller, "Pulse energy scaling to 5 µJ from a femtosecond thin disk laser," *Opt. Lett.*, vol. 31, no. 18, pp. 2728–2730, Sep. 2006.

[85] S. V. Marchese *et al.*, "Femtosecond thin disk laser oscillator with pulse energy beyond the 10-microjoule level," *Opt. Express*, vol. 16, no. 9, pp. 6397–6407, 2008.

[86] J. Neuhaus *et al.*, "Passively mode-locked Yb:YAG thin-disk laser with pulse energies exceeding 13 uJ by use of an active multipass geometry," *Opt. Lett.*, vol. 33, no. 7, pp. 726–728, 2008.

[87] C. R. Baer *et al.*, "Femtosecond Yb:Lu_2O_3 thin disk laser with 63 W of average power," *Opt. Lett.*, vol. 34, no. 18, pp. 2823–2825, Sep. 2009.

[88] O. Pronin *et al.*, "High-power 200 fs Kerr-lens mode-locked Yb:YAG thin-disk oscillator," *Opt. Lett.*, vol. 36, no. 24, pp. 4746–4748, Dec. 2011.

[89] C. J. Saraceno *et al.*, "Sub-100 femtosecond pulses from a SESAM modelocked thin disk laser," *Appl. Phys. B*, vol. 106, no. 3, pp. 559–562, Jan. 2012.

[90] C. Schriber *et al.*, "Pushing SESAM modelocked thin-disk lasers to shortest pulse durations," presented at the Adv. Solid State Lasers Congr., 2014, Paper AF1A.4. [Online]. Available: https://www.osapublishing.org/abstract.cfm?uri=ASSL-2014-AF1A.4

[91] C. Schriber *et al.*, "Dual-gain SESAM mode locked thin disk laser based on Yb:Lu_2O_3 and Yb:Sc_2O_3," *Opt. Express*, vol. 22, no. 16, pp. 18979–18986, Aug. 2014.

[92] A. Diebold *et al.*, "SESAM mode-locked Yb:$CaGdAlO_4$ thin disk laser with 62 fs pulse generation," *Opt. Lett.*, vol. 38, no. 19, pp. 3842–3845, Oct. 2013.

[93] S. Ricaud *et al.*, "Femtosecond Yb:$CaGdAlO_4$ thin-disk oscillator," *Opt. Lett.*, vol. 37, no. 19, pp. 3984–3986, Oct. 2012.

[94] A. A. Eilanlou, Y. Nabekawa, M. Kuwata-Gonokami, and K. Midorikawa, "Femtosecond laser pulses in a Kerr lens mode-locked thin-disk ring oscillator with an intra-cavity peak power beyond 100 MW," *Jpn. J. Appl. Phys.*, vol. 53, no. 8, Aug. 2014, Art. no. 082701.

[95] S. V. Marchese *et al.*, "Efficient femtosecond high power Yb:Lu_2O_3 thin disk laser," *Opt. Express*, vol. 15, no. 25, pp. 16966–16971, 2007.

[96] C. R. E. Baer *et al.*, "Femtosecond thin-disk laser with 141 W of average power," *Opt. Lett.*, vol. 35, no. 13, pp. 2302–2304, Jul. 2010.

[97] C. J. Saraceno *et al.*, "Self-referenceable frequency comb from an ultrafast thin disk laser," *Opt. Express*, vol. 20, no. 9, pp. 9650–9656, Apr. 2012.

[98] C. Paradis *et al.*, "Generation of 35-fs pulses from a Kerr lens mode-locked Yb:Lu_2O_3 thin-disk laser," *Opt. Express*, vol. 25, no. 13, pp. 14918–14925, Jun. 2017.

[99] I. Graumann *et al.*, "High-power mode locked Yb:Lu_2O_3 thin-disk laser with 10-MW sub-500 fs pulses," presented at the Adv. Solid State Lasers, 2016, Paper ATu1A.3. [Online]. Available: https://www.osapublishing.org/abstract.cfm?uri=ASSL-2016-ATu1A.3

[100] G. Palmer *et al.*, "Passively mode-locked Yb:$KLu(WO_4)_2$ thin-disk oscillator operated in the positive and negative dispersion regime," *Opt. Lett.*, vol. 33, no. 14, pp. 1608–1610, Jul. 2008.

[101] A. M. Kowalevicz *et al.*, "Generation of 150-nJ pulses from a multiple-pass cavity Kerr-lens mode-locked Ti:Al_2O_3 oscillator," *Opt. Lett.*, vol. 28, no. 17, pp. 1597–1599, Sep. 2003.

[102] A. Greborio, A. Guandalini, and J. Aus der Au, "Sub-100 fs pulses with 12.5-W from Yb: CALGO based oscillators," *Proc. SPIE*, vol. 8235, 2012, Art. no. 823511.

[103] S. Manjooran and A. Major, "Diode-pumped 45 fs Yb:CALGO laser oscillator with 1.7 MW of peak power," *Opt. Lett.*, vol. 43, no. 10, pp. 2324–2327, May 2018.

[104] M. Gaponenko *et al.*, "Compact megahertz coherent XUV generation by HHG inside an ultrafast thin disk laser," presented at the Nonlinear Opt., 2017, Paper NTh3A.1. [Online]. Available: https://www.osapublishing.org/abstract.cfm?uri=NLO-2017-NTh3A.1

[105] N. Kanda *et al.*, "Multi-port intra-cavity high harmonic generation in a Yb: YAG thin disk mode-locked oscillator with MHz repetition rate," presented at the Front. Opt., 2017, Paper LW5F.4. [Online]. Available: https://www.osapublishing.org/abstract.cfm?uri=LS-2017-LW5F.4

[106] U. Keller *et al.*, "Semiconductor saturable absorber mirrors (SESAM's) for femtosecond to nanosecond pulse generation in solid-state lasers," *IEEE J. Sel. Topics Quantum Electron.*, vol. 2, no. 3, pp. 435–453, Sep. 1996.

[107] C. Kränkel, "Rare-earth-doped sesquioxides for diode-pumped high-power lasers in the 1-, 2-, and 3-µm spectral range," *IEEE J. Sel. Topics Quantum Electron.*, vol. 21, no. 1, Jan. 2015, Art. no. 1602013.

[108] C. G. E. Alfieri *et al.*, "Improved SESAMs for femtosecond pulse generation approaching the kW average power regime," *Opt. Express*, vol. 24, no. 24, Nov. 2016, Art. no. 27587.

[109] C. J. Saraceno *et al.*, "SESAMs for high-power oscillators: Design guidelines and damage thresholds," *IEEE J. Sel. Topics Quantum Electron.*, vol. 18, no. 1, pp. 29–41, Jan./Feb. 2012.

[110] A. Comby *et al.*, "Absolute gas density profiling in high-order harmonic generation," *Opt. Express*, vol. 26, no. 5, pp. 6001–6009, Mar. 2018.

[111] E. D. Palik, *Handbook of Optical Constants of Solids*. New York, NY, USA: Academic, 1997.

[112] C. J. Saraceno *et al.*, "Cutting-edge high-power ultrafast thin disk oscillators," *Appl. Sci.*, vol. 3, no. 2, pp. 355–395, Apr. 2013.

[113] D. C. Yost, "Development of an extreme ultraviolet frequency comb for precision spectroscopy," Ph.D. dissertation, Dept. Phys., Univ. Colorado, Boulder, CO, USA, 2011.

[114] P. Salières *et al.*, "Feynman's path-integral approach for intense-laser-atom interactions," *Science*, vol. 292, no. 5518, pp. 902–905, May 2001.

[115] F. Lindner *et al.*, "High-order harmonic generation at a repetition rate of 100 kHz," *Phys. Rev. A*, vol. 68, no. 1, Jul. 2003, Art. no. 013814.

[116] T. J. Hammond, A. K. Mills, and D. J. Jones, "Near-threshold harmonics from a femtosecond enhancement cavity-based EUV source effects of multiple quantum pathways on spatial profile and yield," *Opt. Express*, vol. 19, no. 25, pp. 24871–24883, 2011.

[117] J. L. Krause, K. J. Schafer, and K. C. Kulander, "High-order harmonic generation from atoms and ions in the high intensity regime," *Phys. Rev. Lett.*, vol. 68, no. 24, pp. 3535–3538, 1992.

[118] M. Lewenstein, P. Balcou, M. Y. Ivanov, A. L'huillier, and P. B. Corkum, "Theory of high-harmonic generation by low-frequency laser fields," *Phys. Rev. A*, vol. 49, no. 3, pp. 2117–2132, 1994.

[119] P. B. Corkum, "Plasma perspective on strong field multiphoton ionization," *Phys. Rev. Lett.*, vol. 71, no. 13, pp. 1994–1997, Sep. 1993.

[120] C. M. Heyl, C. L. Arnold, A. Couairon, and A. L'Huillier, "Introduction to macroscopic power scaling principles for high-order harmonic generation," *J. Phys. B, At., Mol. Opt. Phys.*, vol. 50, no. 1, Jan. 2017, Art. no. 013001.

[121] S. Kazamias *et al.*, "Pressure-induced phase matching in high-order harmonic generation," *Phys. Rev. A*, vol. 83, no. 6, Jun. 2011, Art. no. 063405.

[122] A. Paul *et al.*, "Phase-matching techniques for coherent soft X-ray generation," *IEEE J. Quantum Electron.*, vol. 42, no. 1, pp. 14–26, Jan. 2006.

[123] E. Constant *et al.*, "Optimizing high harmonic generation in absorbing gases: Model and experiment," *Phys. Rev. Lett.*, vol. 82, no. 8, pp. 1668–1671, 1999.

[124] S. Hädrich *et al.*, "Single-pass high harmonic generation at high repetition rate and photon flux," *J. Phys. B, At., Mol. Opt. Phys.*, vol. 49, no. 17, Sep. 2016, Art. no. 172002.

[125] R. Grange *et al.*, "New regime of inverse saturable absorption for self-stabilizing passively mode-locked lasers," *Appl. Phys. B*, vol. 80, no. 2, pp. 151–158, Feb. 2005.

[126] K. Hasse, T. Calmano, B. Deppe, C. Liebald, and C. Kränkel, "Efficient Yb^{3+}:$CaGdAlO_4$ bulk and femtosecond-laser-written waveguide lasers," *Opt. Lett.*, vol. 40, no. 15, pp. 3552–3555, Aug. 2015.

[127] A. Diebold *et al.*, "Optimized SESAMs for kilowatt-level ultrafast lasers," *Opt. Express*, vol. 24, no. 10, pp. 10512–10526, May 2016.

[128] U. Keller, "Ultrafast solid-state laser oscillators: A success story for the last 20 years with no end in sight," *Appl. Phys. B*, vol. 100, no. 1, pp. 15–28, Jul. 2010.

[129] A. Klenner, S. Schilt, T. Südmeyer, and U. Keller, "Gigahertz frequency comb from a diode-pumped solid-state laser," *Opt. Express*, vol. 22, no. 25, pp. 31008–31019, Dec. 2014.

[130] T. D. Shoji *et al.*, "Ultra-low-noise monolithic mode-locked solid-state laser," *Optica*, vol. 3, no. 9, pp. 995–998, Sep. 2016.

[131] A. S. Mayer, C. R. Phillips, and U. Keller, "Watt-level 10-gigahertz solid-state laser enabled by self-defocusing nonlinearities in an aperiodically poled crystal," *Nature Commun.*, vol. 8, no. 1, Dec. 2017, Art. no. 1673.

[132] J. Zhang *et al.*, "49-fs Yb: YAG thin-disk oscillator with distributed Kerr-lens mode-locking," presented at the Eur. Conf. Lasers Electro-Opt.-Eur. Quantum Electron. Conf., 2015, Paper PD_A_1. [Online]. Available: https://www.osapublishing.org/abstract.cfm?uri=CLEO_Europe-2015-PD_A_1

[133] J. Zhang *et al.*, "Multi-mW, few-cycle mid-infrared continuum spanning from 500 to 2250 cm−1," *Light, Sci. Appl.*, vol. 7, no. 2, Feb. 2018, Art. no. 17180. [Online]. Available: https://www.osapublishing.org/abstract.cfm?uri=CLEO_Europe-2015-PD_A_1

[134] F. Saltarelli, A. Diebold, I. J. Graumann, C. R. Phillips, and U. Keller, "Mode locking of a thin-disk laser with the frequency-doubling nonlinear-mirror technique," *Opt. Express*, vol. 25, no. 19, pp. 23254–23266, Sep. 2017.

[135] K. Moll, R. Jones, and J. Ye, "Nonlinear dynamics inside femtosecond enhancement cavities," *Opt. Express*, vol. 13, no. 5, pp. 1672–1678, Mar. 2005.

[136] C. M. Heyl, S. B. Schoun, G. Porat, H. Green, and J. Ye, "A nozzle for high-density supersonic gas jets at elevated temperatures," *Rev. Sci. Instrum.*, vol. 89, no. 11, Nov. 2018, Art. no. 113114.

[137] D. Esser *et al.*, "Laser-manufactured mirrors for geometrical output coupling of intracavity-generated high harmonics," *Opt. Express*, vol. 21, no. 22, pp. 26797–26805, Nov. 2013.

[138] J. Weitenberg, P. Rußbüldt, T. Eidam, and I. Pupeza, "Transverse mode tailoring in a quasi-imaging high-finesse femtosecond enhancement cavity," *Opt. Express*, vol. 19, no. 10, pp. 9551–9561, May 2011.

[139] I. Pupeza *et al.*, "Cavity-enhanced high-harmonic generation with spatially tailored driving fields," *Phys. Rev. Lett.*, vol. 112, no. 10, Mar. 2014, Art. no. 103902.

[140] F. Merkt and T. P. Softley, "Final-state interactions in the zero-kinetic-energy-photoelectron spectrum of H_2," *J. Chem. Phys.*, vol. 96, no. 6, pp. 4149–4156, Mar. 1992.

[141] M. Herrmann *et al.*, "Feasibility of coherent XUV spectroscopy on the 1 S − 2 S transition in singly ionized helium," *Phys. Rev. A*, vol. 79, no. 5, May 2009, Art. no. 052505.

[142] E. E. Eyler *et al.*, "Prospects for precision measurements of atomic helium using direct frequency comb spectroscopy," *Eur. Phys. J. D*, vol. 48, no. 1, pp. 43–55, Jun. 2008.

[143] M. T. Murphy, J. K. Webb, and V. V. Flambaum, "Further evidence for a variable fine-structure constant from Keck/HIRES QSO absorption spectra," *Monthly Notices Roy. Astron. Soc.*, vol. 345, no. 2, pp. 609–638, Oct. 2003.

[144] J. C. Berengut, V. A. Dzuba, V. V. Flambaum, and A. Ong, "Electron-hole transitions in multiply charged ions for precision laser spectroscopy and searching for variations in α," *Phys. Rev. Lett.*, vol. 106, no. 21, May 2011, Art. no. 210802.

[145] A. D. Panov, "Quantitative conversion spectroscopy of the ultrasoft isomeric transition of uranium-235 and the electronic structure of uranium oxides," *J. Exp. Theor. Phys.*, vol. 85, no. 2, pp. 313–324, Aug. 1997.

[146] E. Peik and C. Tamm, "Nuclear laser spectroscopy of the 3.5 eV transition in Th-229," *Europhys. Lett.*, vol. 61, no. 2, pp. 181–186, Jan. 2003.

[147] W. G. Rellergert *et al.*, "Constraining the evolution of the fundamental constants with a solid-state optical frequency reference based on the Th-229 nucleus," *Phys. Rev. Lett.*, vol. 104, no. 20, May 2010, Art. no. 200802.

[148] C. J. Campbell, A. G. Radnaev, and A. Kuzmich, "Wigner crystals of Th 229 for optical excitation of the nuclear isomer," *Phys. Rev. Lett.*, vol. 106, no. 22, Jun. 2011, Art. no. 223001.

[149] C. J. Campbell *et al.*, "Single-ion nuclear clock for metrology at the 19th decimal place," *Phys. Rev. Lett.*, vol. 108, no. 12, Mar. 2012, Art. no. 120802.

[150] L. von der Wense *et al.*, "Direct detection of the 229Th nuclear clock transition," *Nature*, vol. 533, no. 7601, pp. 47–51, May 2016.

[151] A. Klenner *et al.*, "Phase-stabilization of the carrier-envelope-offset frequency of a SESAM mode locked thin disk laser," *Opt. Express*, vol. 21, no. 21, pp. 24770–24780, Oct. 2013.

[152] O. Pronin *et al.*, "Carrier-envelope phase stabilized thin-disk oscillator," in *Proc. Adv. Solid-State Lasers Congr.*, 2013, Paper AF3A.5.

[153] M. Seidel *et al.*, "Carrier-envelope-phase stabilization via dual wavelength pumping," *Opt. Lett.*, vol. 41, no. 8, pp. 1853–1856, Apr. 2016.

[154] S. Gröbmeyer, J. Brons, M. Seidel, and O. Pronin, "100 W-level carrier-envelope-phase stable thin-disk oscillator," presented at the 8th EPS-QEOD Europhoton Conf., Barcelona, Spain, 2018, Paper FrM2.2.

[155] N. Modsching *et al.*, "Carrier-envelope offset frequency stabilization of a thin-disk laser oscillator operating in the strongly self-phase modulation broadened regime," *Opt. Express*, vol. 26, no. 22, pp. 28461–28467, Oct. 2018.

[156] A. Schliesser, N. Picqué, and T. W. Hänsch, "Mid-infrared frequency combs," *Nature Photon.*, vol. 6, no. 7, pp. 440–449, Jul. 2012.

[157] D. T. Reid *et al.*, "Roadmap on ultrafast optics," *J. Opt.*, vol. 18, no. 9, Sep. 2016, Art. no. 093006.

[158] O. Pronin *et al.*, "High-power multi-megahertz source of waveform-stabilized few-cycle light," *Nature Commun.*, vol. 6, May 2015, Art. no. 6988.

[159] J. M. Dudley and S. Coen, "Coherence properties of supercontinuum spectra generated in photonic crystal and tapered optical fibers," *Opt. Lett.*, vol. 27, no. 13, pp. 1180–1182, Jul. 2002.

[160] S. Koke, A. Anderson, H. Frei, A. Assion, and G. Steinmeyer, "Noise performance of a feed-forward scheme for carrier-envelope phase stabilization," *Appl. Phys. B*, vol. 104, no. 4, pp. 799–804, Sep. 2011.

[161] M. Hoffmann, S. Schilt, and T. Südmeyer, "CEO stabilization of a femtosecond laser using a SESAM as fast opto-optical modulator," *Opt. Express*, vol. 21, no. 24, pp. 30054–30064, Dec. 2013.

[162] S. Hakobyan *et al.*, "Carrier-envelope offset stabilization of a GHz repetition rate femtosecond laser using opto-optical modulation of a SESAM," *Opt. Lett.*, vol. 42, no. 22, pp. 4651–4654, Nov. 2017.

[163] K. Gürel, S. Hakobyan, V. J. Wittwer, S. Schilt, and T. Südmeyer, "Frequency comb stabilization of ultrafast lasers by opto-optical modulation of semiconductors," *IEEE J. Sel. Topics Quantum Electron.*, vol. 24, no. 5, Sep. 2018, Art. no. 1102309.

[164] G. Di Domenico, S. Schilt, and P. Thomann, "Simple approach to the relation between laser frequency noise and laser line shape," *Appl. Opt.*, vol. 49, no. 25, pp. 4801–4807, 2010.

[165] N. Modsching *et al.*, "Frequency comb stabilization of a 50-fs thin-disk laser oscillator operating in a strongly SPM-broadened regime," presented at the Conf. Lasers Electro-Opt., 2018, Paper SM4L.6.

[166] F. Emaury *et al.*, "Frequency comb offset dynamics of SESAM mode locked thin disk lasers," *Opt. Express*, vol. 23, no. 17, pp. 21836–21856, Aug. 2015.

[167] M. Gaponenko *et al.*, unpublished.

[168] M. Gaponenko *et al.*, "CEO frequency stabilization of a thin disk laser with intra-cavity high harmonic generation," presented at the 8th EPS-QEOD Europhoton Conf., Barcelona, Spain, 2018, Paper FrM2.6.

François Labaye was born in France in 1986. He studied at Université Bordeaux 1 where he obtained his master's in physics in 2009. In parallel to his master degree, he studied for eight months at CREOL, The College of Optics and Photonics of the University of Central Florida (Orlando, USA), where he did an internship in the group of Prof. Martin C. Richardson. He did his Ph.D in the group of Prof. Fabian Zomer at the Laboratoire de l'accélérateur linéaire, Université Paris Sud 11, on "Passive enhancement of fiber laser in a Fabry.Pérot cavity: Application to gamma-rays production by Compton backscattering" and graduated in 2012. He then moved to the group of Prof. Jun Ye at JILA (Boulder, USA) where he worked on the development of XUV frequency combs based on passive enhancement cavities. In 2015, he joined the group of Prof. Thomas Südmeyer at the University of Neuchâtel, Switzerland, as a Postdoctoral Fellow. His current research interests are the development of novel XUV sources and frequency combs.

Maxim Gaponenko was born in Belarus in 1980. He studied with the Physics Faculty and received the graduate degree with honors in 2003 from Belarusian State University, Minsk, Belarus, and the Ph.D. degree from Belarusian National Technical University, Minsk, Belarus, in 2011. In 2012, he joined the group of Prof. T. Südmeyer with the University of Neuchâtel, Neuchâtel, Switzerland. He is a coauthor of 25 papers in peer-reviewed journals. His current research interests include the development of novel ultrafast laser sources and the investigation of nonlinear optical phenomena.

Norbert Modsching was born in Hoyerswerda, Germany, in 1986. He received the M.S. degree in photonics from Friedrich-Schiller University Jena, Jena, Germany, in 2014 and the Ph.D. degree from Laboratoire Temps-Fréquence (LTF), University of Neuchâtel, Neuchâtel, Switzerland, in 2019. Since 2015, he has been in the group of Prof. T. Südmeyer with the Laboratoire Temps-Fréquence (LTF), University of Neuchâtel, Neuchâtel, Switzerland, where he continues his research as a Postdoctoral Scientist.

During his master studies, he was with the Institute of Applied Physics, Jena, Germany, in the group of Prof. J. Limpert, where he worked on high-power rod-type fiber amplifier and mode instabilities. He has authored or coauthored more than ten articles in international peer-reviewed journals and more than 40 conference contributions. His current research interests at the LTF focus on power scaling of ultrafast thin-disk laser oscillators in the sub-100-fs pulse duration regime and their subsequent application as frequency comb, for THz generation and for intraoscillator high harmonic generation.

Dr. Modsching has been awarded two times for his student paper contributions on international conferences.

Pierre Brochard was born in Versailles, France, in 1992. He studied physics and received the M.S. degree with highest honors in 2015 from Université du Maine, Le Mans, France. Since 2015, he has been working toward the Ph.D. degree with the Laboratoire Temps-Fréquence, University of Neuchâtel, Neuchâtel, Switzerland, where he works on optical frequency combs and frequency stabilized lasers.

He is the author or coauthor of 13 articles in international peer-reviewed journals and more than 35 conference contributions. He has been once awarded and three times finalist for his student paper contributions at international conferences.

Clément Paradis was born in Grenoble, France, in 1989. He received the "Diplôme d'Ingénieur" (engineering diploma equivalent to the master's degree) from Ecole Nationale Supérieur de Techniques Avancées ParisTech, Palaiseau, France (member of the ParisTech Network–Université Paris-Saclay), in 2013, the master's degree in the framework of the European Erasmus Mundus Program Optics in Science and Technology in 2013, and the M.Sc. degrees in photonics in the framework of the European Erasmus Mundus Program Optics in Science and Technology from the Friedrich-Schiller University of Jena, Jena, Germany, and the Imperial College of London, London, U.K., and the Ph.D. degree for his work entitled "Novel ultrafast high-power thin-disk laser oscillators and applications for metrology and XUV generation" in 2018. In the same year, he joined the research group of Prof. T. Südmeyer with the Laboratoire Temps-Fréquence (LTF), University of Neuchâtel, Switzerland. He received the Ph.D. degree in 2018 for his work entitled "Novel ultrafast high-power thin-disk laser oscillators and applications for metrology and XUV generation".

After his graduation, he continued his research as a Postdoctoral Scientist with the LTF. His investigations mainly focus on the development of high-power ultrafast laser sources based on thin-disk laser oscillators and subsequent applications. He has authored or coauthored six articles in international peer-reviewed journals and more than 40 conference contributions.

Dr. Paradis is a member of the Optical Society of America.

Stéphane Schilt was born in Lausanne, Switzerland, in 1970. He received the M.S. degree in physics and the Ph.D. degree in technical sciences from the Swiss Federal Institute of Technology Lausanne (EPFL), Lausanne, Switzerland, in 1994 and 2002, respectively.

From 2002 to 2005, he was a Postdoc with EPFL. Then, he joined as a Project Manager with IR Microsystems, Lausanne, where he worked on the development of laser-based trace gas sensors. Since 2009, he has been a Senior Scientist with the Laboratoire Temps-Fréquence, University of Neuchâtel, Switzerland. He has authored or coauthored two book chapters, more than 60 articles in international peer-reviewed journals, and more than 140 conference contributions. His research interests include optical frequency combs, optical metrology, frequency-stabilized lasers, and laser spectroscopy. He is an Associate Editor for the *Journal of Spectroscopy*, and acts as a Reviewer for various journals. He holds or has applied for four patents.

Dr. Schilt is a member of the Optical Society of America, the Swiss Physical Society, and the European Physical Society. He was also a member of the Optical Metrology Committee for the CLEO Conference (2015–2017) and is a committee member for the LACSEA conference (2016–2020).

Valentin Johannes Wittwer was born in Switzerland, in 1983. He received the Diploma in physics and the Ph.D. degree from the Federal Institute of Technology (ETH), Zurich, Switzerland, in 2008 and 2012, respectively. His Ph.D. work was realized in the group of Prof. U. Keller, where he worked on the development of ultrafast semiconductor lasers.

Then, he joined the group of Prof. T. Sdmeyer with the University of Neuchâtel.

Dr. Wittwer has authored or coauthored more than 30 articles in international peer-reviewed journals, and more than 80 conference contributions. As a Senior Scientist, he is currently leading the ion-beam sputtering growth activities, managing collaborative projects with industry and supporting the ultrafast thin-disk laser and frequency comb activities. He has been awarded a fellowship by the Swiss National Science Foundation to do a postdoc with the University of Cambridge, Cambridge, U.K., in the group of Prof. A. C. Ferrari, where he was developing graphene-based saturable absorbers for ultrafast lasers.

Thomas Südmeyer studied physics at Leibniz University, Hanover, Germany, and Ecole Normale Superieure, Paris, France, and received the Ph.D. degree in 2003 from Eidgenössische Technische Hochschule (ETH), Zurich, Switzerland, for research on the first mode-locked thin-disk lasers and novel nonlinear systems.

In 1999, he started working on ultrafast lasers during an EU fellowship with the Strathclyde University, Glasgow. From 2003 to 2005, he developed industrial laser solutions with Sony Corporation, Tokyo. From 2005 to 2011, in his habilitation, he investigated new concepts for ultrafast science and technology with ETH Zurich, Switzerland. In 2011, he was appointed as a Full Professor and the Head of the Laboratoire Temps-Fréquence with the University of Neuchâtel, Switzerland. He has been the Coordinator of several Swiss and European Projects and was awarded with an ERC Starting Grant. He has been serving the research community as an Associate Editor for *Optics Express* (2009–2015) and for IEEE PHOTONICS TECHNOLOGY LETTERS 2014 to 2017. He is the author of more than 110 papers in international peer-reviewed journals, two book chapters, and he holds or has applied for 11 patents. In 2018, he was elected into the National Research Council of the Swiss National Science Foundation (SNSF). His research interests are exploring and pushing the frontiers in photonics, metrology, and ultrafast science.